

THE ACTIVITY OF ZINC OXIDE IN MULTICOMPONENT SLAGS

by

WILLIAM GEORGE DAVENPORT

A THESIS SUBMITTED IN PARTIAL FULFILMENT
OF THE REQUIREMENTS FOR THE DEGREE OF
MASTER OF APPLIED SCIENCE
IN THE DEPARTMENT
OF
MINING AND METALLURGY

We accept this thesis as conforming to the
standard required from candidates for
the degree of MASTER OF APPLIED SCIENCE

Members of the Department of Mining and Metallurgy

THE UNIVERSITY OF BRITISH COLUMBIA

August, 1960.

In presenting this thesis in partial fulfilment of the requirements for an advanced degree at the University of British Columbia, I agree that the Library shall make it freely available for reference and study. I further agree that permission for extensive copying of this thesis for scholarly purposes may be granted by the Head of my Department or by his representatives. It is understood that copying or publication of this thesis for financial gain shall not be allowed without my written permission.

Department of Mining and Metallurgy

The University of British Columbia,
Vancouver 8, Canada.

Date August 15th, 1960.

ABSTRACT

The activity of zinc oxide in multicomponent slags has been investigated. Activities were determined experimentally by equilibrating iron saturated brasses with slags containing iron oxide. Required activities in the Zn-Cu-Fe system were obtained from experimental iron saturation data and available information on the Zn-Cu and Cu-Fe systems.

Where measurement was not possible, thermodynamic analyses of slag systems were carried out.

Rigid activity patterns in the ZnO-SiO₂, ZnO-FeO-SiO₂, ZnO-CaO-SiO₂ and ZnO-FeO-CaO-SiO₂ systems have been developed from experimental and analytical data.

Agreement with the activity data of Bell, Turner and Peters on ZnO-FeO-CaO-SiO₂ and Okunev and Bovykin on ZnO-FeO-SiO₂ type slags indicates that the present measurement technique provides a good basis for industrial slag investigations.

ACKNOWLEDGEMENT

The author gratefully acknowledges Dr. C. S. Samis and Mrs. A. M. Armstrong for their assistance and encouragement. It is a pleasure to acknowledge Mr. G. W. Toop for many profitable discussions of the work.

The author wishes to thank the Consolidated Mining and Smelting Company of Canada Limited for kindly carrying out the analyses of the slags investigated.

Thanks are also due to the Defence Research Board and the National Research Council of Canada for financial support of the research.

TABLE OF CONTENTS

	<u>Page</u>
I. INTRODUCTION	1
Object and Scope of the Present Investigation	2
II. METHOD OF ACTIVITY MEASUREMENT	3
A. Iron Activity	4
B. Zinc Activity	4
1. Methods of Thermodynamic Analysis	4
2. Discussion	7
3. Possible Errors Arising from the Use of Zinc Activities in the Zn-Cu-Fe System	9
C. Activities of Iron Oxide and Zinc Oxide	9
D. Rearrangement of the Equilibrium Constant	11
III. EXPERIMENTAL	12
A. Materials	12
B. Crucibles	12
C. Furnace	12
D. Temperature Control	12
E. Procedure	16
F. Assaying	16
IV. INVESTIGATION OF THE ZnO-FeO-SiO ₂ SYSTEM	17
A. Auxiliary Systems	17
1. FeO-SiO ₂	17
2. ZnO-SiO ₂	20
3. Silica Activities, ZnO-FeO-SiO ₂ System	25

TABLE OF CONTENTS (continued)

	<u>Page</u>
B. Experimental Zinc Oxide Activity Determination, System ZnO-FeO-SiO ₂	25
1. First Approximation, Zinc Oxide Activity Calculation	25
2. Final Determination of Zinc Oxide Activity . .	28
C. Accuracy of Experimental Zinc Oxide Activities . .	28
D. Summary of Thermodynamic Data, ZnO-FeO-SiO ₂ System	31
V. INVESTIGATION OF THE ZnO-FeO-CaO-SiO ₂ SYSTEM	35
A. Auxiliary Systems	35
1. ZnO-FeO-SiO ₂ System	35
2. FeO-CaO-SiO ₂ System	35
3. ZnO-CaO-SiO ₂ System	36
B. Experimental Zinc Oxide Activity Determination, System ZnO-FeO-CaO-SiO ₂	47
VI. COMPARISONS WITH OTHER INVESTIGATIONS	52
A. Richards and Thorne	52
B. Okunev and Bovykin	52
C. Bell, Turner and Peters	54
VII. DISCUSSION	58
VIII. CONCLUSIONS	59
IX. REFERENCES	60
X. APPENDICES	
I. Calculations on the Zn-Cu-Fe System	62
II. Calculation of Activities, System ZnO-SiO ₂	64
III. Determination of Zinc Oxide Activities, System ZnO-FeO-SiO ₂	68

TABLE OF CONTENTS (continued)

	<u>Page</u>
IV. Thermodynamic Analysis of the ZnO-FeO-SiO ₂ System; Calculations	70
V. Thermodynamic Analysis of the ZnO-CaO-SiO ₂ System; Calculations	73
VI. Determination of Zinc Oxide Activities, System ZnO-CaO-FeO-SiO ₂	75

LIST OF FIGURES

<u>Fig. No.</u>		Page
1.	Isoactivity Pattern, Zn-Cu-Fe System, 1300°C	5
2.	Zinc Activity along Iron Saturation Line, Zn-Cu-Fe System, 1300°C	6
3.	Comparison of Regular Solution Plots of Zn-Cu and Fe Saturated Zn-Cu Systems, 1300°C	8
4.	Liquidus Curve, Cu-Fe System	10
5.	Iron Crucible	13
6.	Experimental Furnace	14
7.	Experimental Furnace, Construction Details	15
8.	Activity of Ferrous Oxide in Binary Silicate Melts at 1315°C	18
9.	Activity of SiO ₂ , System FeO-SiO ₂ , 1300°C, calculated from Schuhmann and Ensio	19
10.	Phase Diagram, ZnO-SiO ₂ System	21
11.	The Activities of ZnO and SiO ₂ , ZnO-SiO ₂ System, 1300°C	22
12.	Regular Solution Plots of ZnO, FeO and CaO in Binary Silicate Systems, 1600°C	24
13.	Silica Isoactivity Pattern, ZnO-FeO-SiO ₂ System, 1300°C	26
14.	Experimental Activity Coefficient Ratios, ZnO-FeO-SiO ₂ System, 1300°C	27
15.	Experimental Zinc Oxide Isoactivity Lines, ZnO-FeO-SiO ₂ System, 1300°C	29
15a.	Iron Oxide Activity Pattern, ZnO-FeO-SiO ₂ System, 1300°C	30
16.	Summary of Zinc Oxide Activity Data, ZnO-FeO-SiO ₂ System, 1600°C	32
17.	Summary of Iron Oxide Activity Data, ZnO-FeO-SiO ₂ System, 1600°C	33
18.	Silica Isoactivity Pattern, ZnO-FeO-SiO ₂ System, 1600°C	34
19.	Activities in the CaO-SiO ₂ System, 1600°C	37
20.	Iron Oxide Isoactivity Pattern, FeO-CaO-SiO ₂ System, 1600°C	39

LIST OF FIGURES (continued)

<u>Fig. No.</u>	<u>Page</u>
21. CaO Isoactivity Pattern, FeO-CaO-SiO ₂ System, 1600°C . . .	40
22. Silica Isoactivity Pattern, FeO-CaO-SiO ₂ System, 1600°C . .	41
23. Activities of ZnO and SiO ₂ , ZnO-SiO ₂ System, 1600°C	42
24. Phase Diagram, ZnO-CaO-SiO ₂ System	43
25. Zinc Oxide Isoactivity Pattern, ZnO-CaO-SiO ₂ System, 1600°C	44
26. Lime Isoactivity Pattern, ZnO-CaO-SiO ₂ System, 1600°C . . .	45
27. Silica Isoactivity Pattern, ZnO-CaO-SiO ₂ System, 1600°C . .	46
28. Isoactivity Patterns, ZnO-FeO-CaO-SiO ₂ System, 1600°C, <u>40% SiO₂ Cut</u>	48
29. Isoactivity Patterns, ZnO-FeO-CaO-SiO ₂ System, 1600°C, <u>34% SiO₂ Cut</u>	49
30. Isoactivity Patterns, ZnO-FeO-CaO-SiO ₂ System, 1600°C, <u>21.5% SiO₂ Cut</u>	50
31. Isoactivity Patterns, ZnO-FeO-CaO-SiO ₂ System, 1600°C, <u>13% SiO₂ Cut</u>	51
32. Comparison of Activity Data, ZnO-FeO-SiO ₂ System, 1200°C .	55
33. Comparisons of Activity Data, ZnO-FeO-CaO-SiO ₂ System, 33a. 1200°C	56, 57
34. Integration Paths, Zn-Cu-Fe System	63
35. Regular Solution Plot of SiO ₂ Activity, System ZnO-SiO ₂ , 1600°C	66
36. Integration Paths, ZnO-FeO-SiO ₂ System	71
37. Integration Paths, ZnO-CaO-SiO ₂ System	74

LIST OF TABLES

Table No.		Page
1.	Activities of ZnO and SiO ₂ , ZnO-SiO ₂ System, 1300°C	23
2.	Activities in the CaO-SiO ₂ System, 1600°C	38
3.	Comparison of the Data of Richards and Thorne and the Results of the Present Investigation	53

THE ACTIVITY OF ZINC OXIDE IN MULTICOMPONENT SLAGS

INTRODUCTION

The thermodynamic activity of zinc oxide in metallurgical slags is of industrial significance. Slags containing zinc oxide are produced in several lead and copper smelting processes. Zinc is recovered from these slags by selective reduction processes. The activity of zinc oxide in slags is an important factor in the rate of zinc elimination and the total zinc recovery.

A review of the literature indicates that several investigations of zinc oxide slag systems have been made. The ZnO-SiO₂¹ and the ZnO-CaO-SiO₂² phase diagrams have been evaluated. The entropy of fusion³ and free energy of formation⁴ of Zn₂SiO₄ have been estimated. Three investigations into the activity of zinc oxide in slags have been made^{5,6,7}.

Bell, Turner and Peters⁵ investigated Zinc Fuming Furnace slags, making use of two equilibrium reactions:

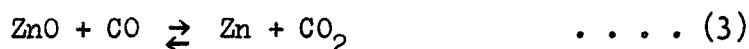


These authors calculated zinc oxide activities from the instantaneous zinc elimination rates and fuel compositions in an operating zinc fuming furnace.

A similar investigation was carried out by Okunev and Bovykin⁶ on the slags from copper and lead processes.

As these investigations were carried out under complex operating conditions, the assumption that equilibrium is reached in these processes has been questioned⁸.

An experimental investigation of zinc oxide slag systems was carried out by Richards and Thorne⁷. Two equilibria were involved:



The slags investigated contained less than two mol per cent zinc oxide.

Object and Scope of the Present Investigation

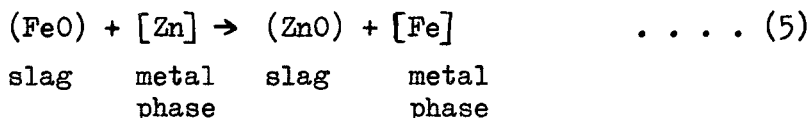
The object of the present investigation is to evaluate the activity of zinc oxide in systems which (i) are basic components of complex slags, or (ii) represent industrial slag compositions. Activities are to be calculated where experimental measurement is not possible, due to (i) excessive melting point temperatures, (ii) high zinc vapour pressures, or (iii) the lack of equilibrium information.

The slags to be studied in this investigation are the ZnO-SiO₂, ZnO-FeO-SiO₂, ZnO-CaO-SiO₂ and ZnO-FeO-CaO-SiO₂ systems.

METHOD OF ACTIVITY MEASUREMENT

The method proposed for the measurement of zinc oxide activities was the equilibration of iron oxide containing slags with an iron saturated Zn-Cu phase.

The equilibrium reaction chosen was:



The equilibrium constant for this reaction has been calculated from existing thermodynamic data^{9,10}.

$$K_{1573^\circ\text{K}} = \frac{(a_{\text{ZnO}_1}) [a_{\text{Fe}}]}{(a_{\text{FeO}_1}) [a_{\text{Zn}}]} = 5.22 \pm 15\%$$

A liquid standard state for zinc oxide was chosen because it provides a more useful criterion for the understanding of liquid slag behaviour. Because no data on the entropy of fusion of zinc oxide was available, an estimate of 2.85 entropy units was made on the basis of activity calculations in the ZnO-SiO₂ system. Whereas the entropy of fusion may be in error, all activity information obtained in the investigation is consistent with this value. The accuracy limits assigned to the equilibrium constant are those determined from the source of existing thermochemical data.

The evaluation of zinc oxide by this equilibrium requires that the activities of FeO, Fe and Zn be known. Experimental conditions were established to provide this information.

A. Iron Activity

The activity of iron was established at unity by the use of an iron crucible for the equilibrium measurements. At equilibrium the metal phase is saturated with γ iron.

B. Zinc Activity

Zinc activities in the iron-saturated brass phase were evaluated from the shape and disposition of the experimental iron saturation line (Figure 1) in conjunction with existing activity information on the Zn-Cu¹¹ and Cu-Fe¹² systems. Iron saturation data were obtained from the experimental metal phase compositions.

Using this basic information, the system was evaluated thermodynamically by the application of Gibbs Duhem integration techniques, and the activities of zinc and copper were calculated along the experimental iron saturation line (Appendix I). The results are shown in Figures 1 and 2.

1. Methods of Thermodynamic Analysis

Three different methods of thermodynamic analysis were employed in the calculation of zinc activities. These techniques were also used in later examinations of ternary slag systems.

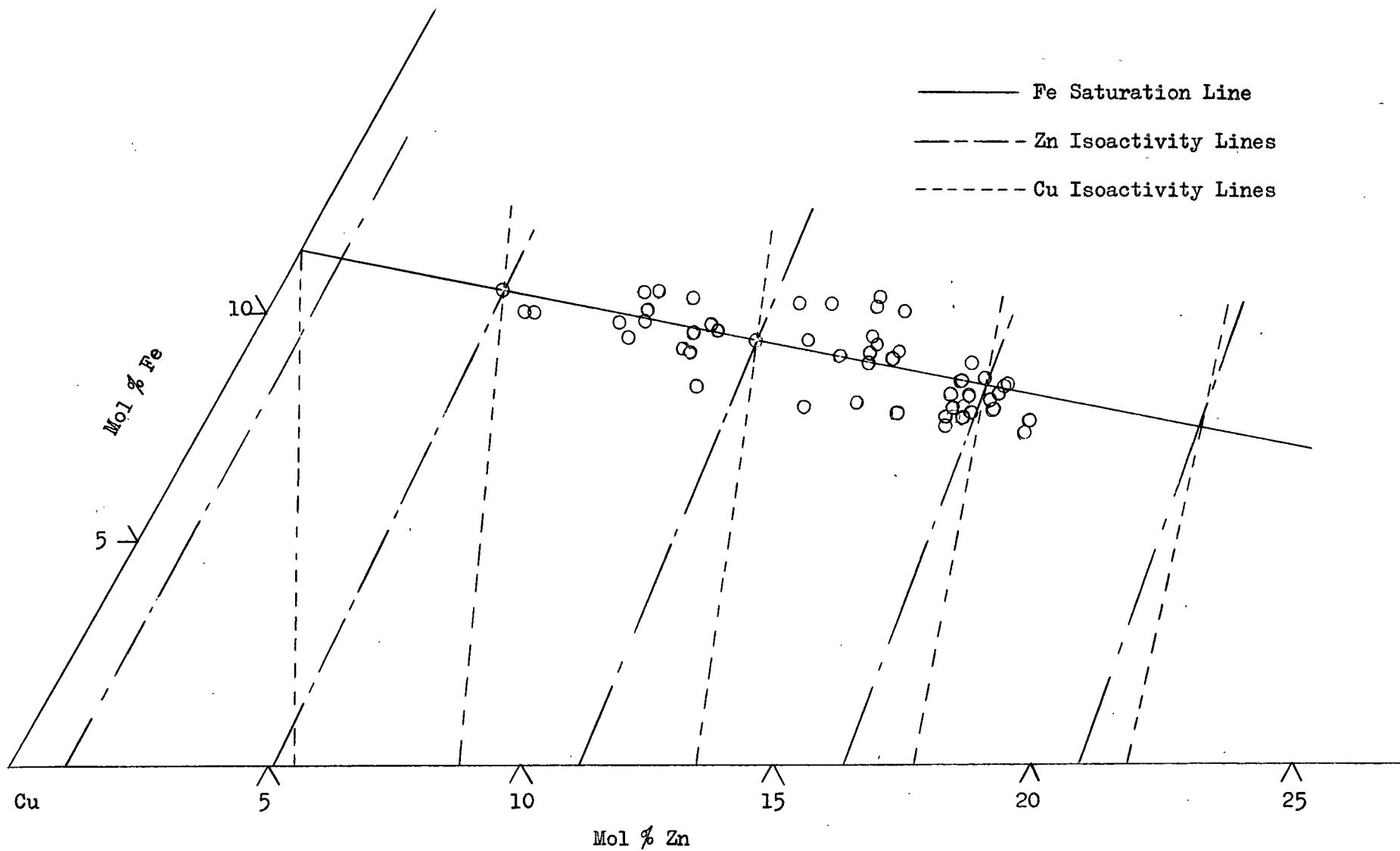


Figure 1. Isoactivity Pattern, Zn-Cu-Fe System, 1300°C.

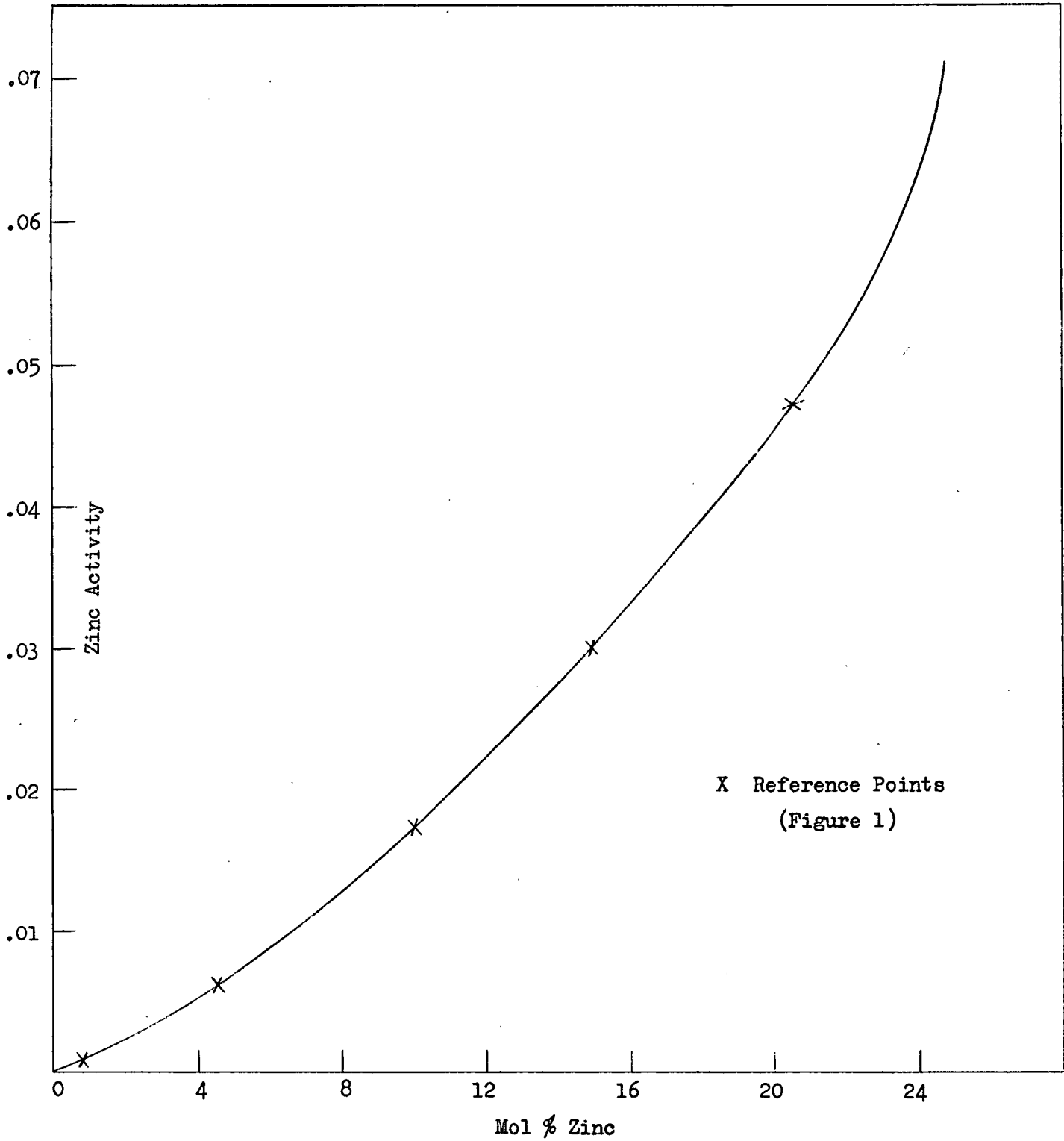


Figure 2. Zinc Activity along Iron Saturation Line,
System Zn-Cu-Fe, 1300°C.

- 1) Schuhmann's graphical application of the Gibbs Duhem equation¹³.
- 2) Schuhmann's ternary intercept Gibbs Duhem integration¹⁴, i.e.

$$\text{Lna}_2 = - \left(\int \left(\frac{\partial N_1}{\partial N_2} \right)_{(a_1, N_3)} d\text{Lna}_1 \right)_{N_2/N_3}$$

- 3) The basic Gibbs Duhem integration application along an iso-activity line, i.e.

$$d\text{Lna}_2 = - \frac{N_1}{N_2} d\text{Lna}_1 \quad (a_3 = \text{constant})$$

The employment of these three analytical techniques provided the means by which experimental iron saturation data and available binary activity information could be utilized in the evaluation and verification of zinc activities in the Zn-Cu-Fe system (Appendix I).

2. Discussion

The effect of iron saturation on zinc and copper activities appears to be slight. Figure 3 shows a comparison of regular solution plots of the binary (Everett, Jacobs and Kitchener¹¹, 1300°C) and iron saturated Zn-Cu systems. Everett, Jacobs and Kitchener showed the binary system to be completely regular. The calculation of the iron saturated system shows that although the zinc activity coefficient is raised the system exhibits near regular solution behaviour.

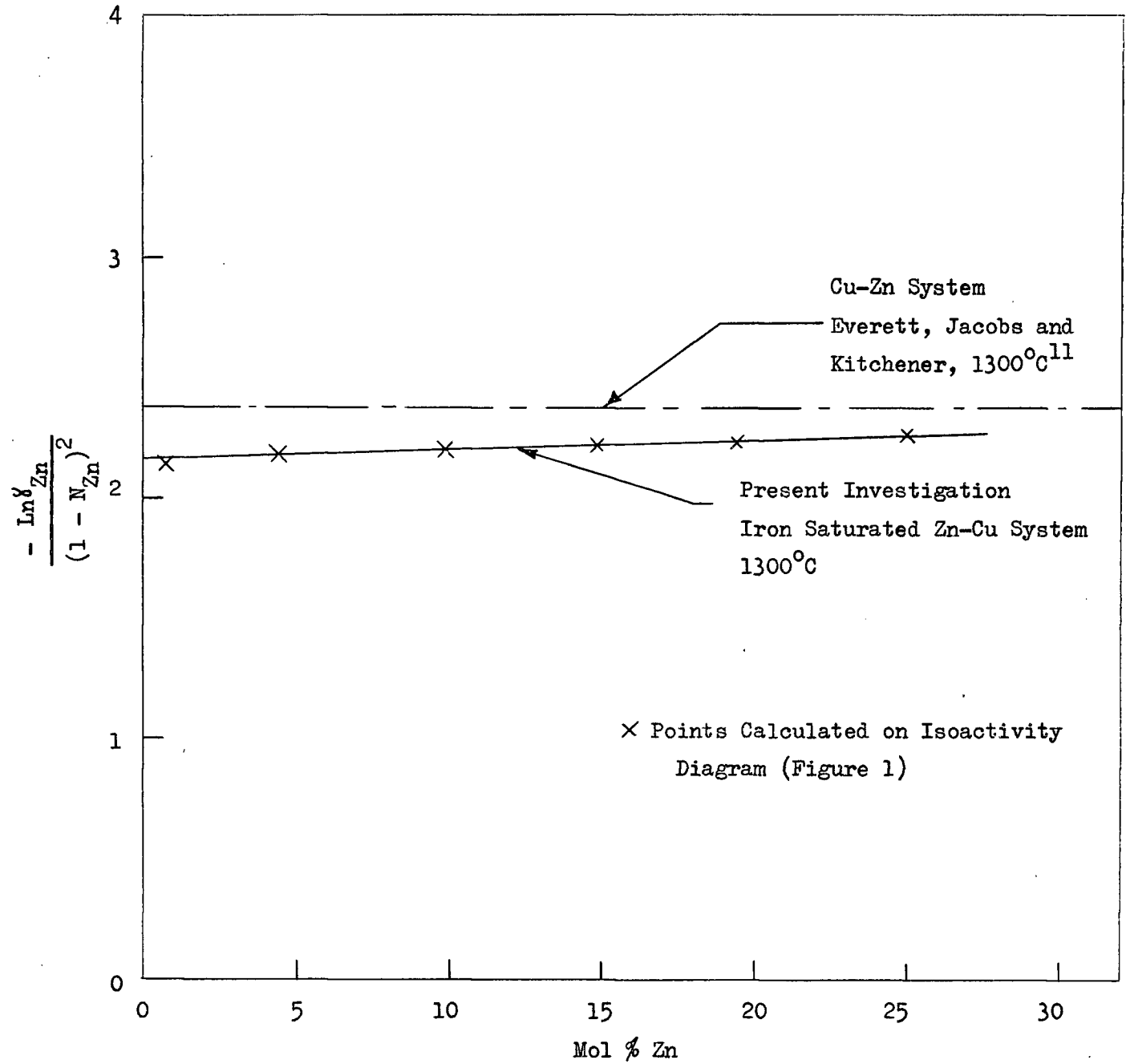


Figure 3, Comparison of Regular Solution Plots of Zn-Cu and Fe Saturated Zn-Cu Systems, 1300°C.

3. Possible Errors Arising from the Use of Zinc Activities in the Zn-Cu-Fe System

The total errors introduced by the use of zinc activities in the ternary metal phase were estimated at $\pm 16\%$.

Everett, Jacobs and Kitchener¹¹ report their experimental error to be less than $\pm 1\%$. Assaying errors in the present investigation are given at $\pm 3\%$.

Temperature errors have a twofold effect. Because of the high temperature dependence of the Fe saturation composition in the Cu-Fe¹⁵ system (Figure 4), the ternary Fe saturation line may vary up to $\pm .8$ mol per cent Fe with a $\pm 10^\circ\text{C}$ variation. Temperature variations also cause a small direct effect on zinc activity. Within the temperature accuracy given ($\pm 10^\circ\text{C}$) the total temperature effect on zinc activities was estimated to be $\pm 2\%$.

Calculation errors were assigned on the basis of detectable variations in the isoactivity pattern. Because of the rigidity of the pattern developed by the three Gibbs Duhem integration methods, and because of the relatively small amounts of iron present, calculation error limits were estimated at $\pm 10\%$.

C. Activities of Iron Oxide and Zinc Oxide

Because the activity values of iron oxide are required in the measurements of zinc oxide activities, these two components must exist in a common slag phase. A method was developed whereby available information on auxiliary slag systems could be used to evaluate zinc oxide activities in

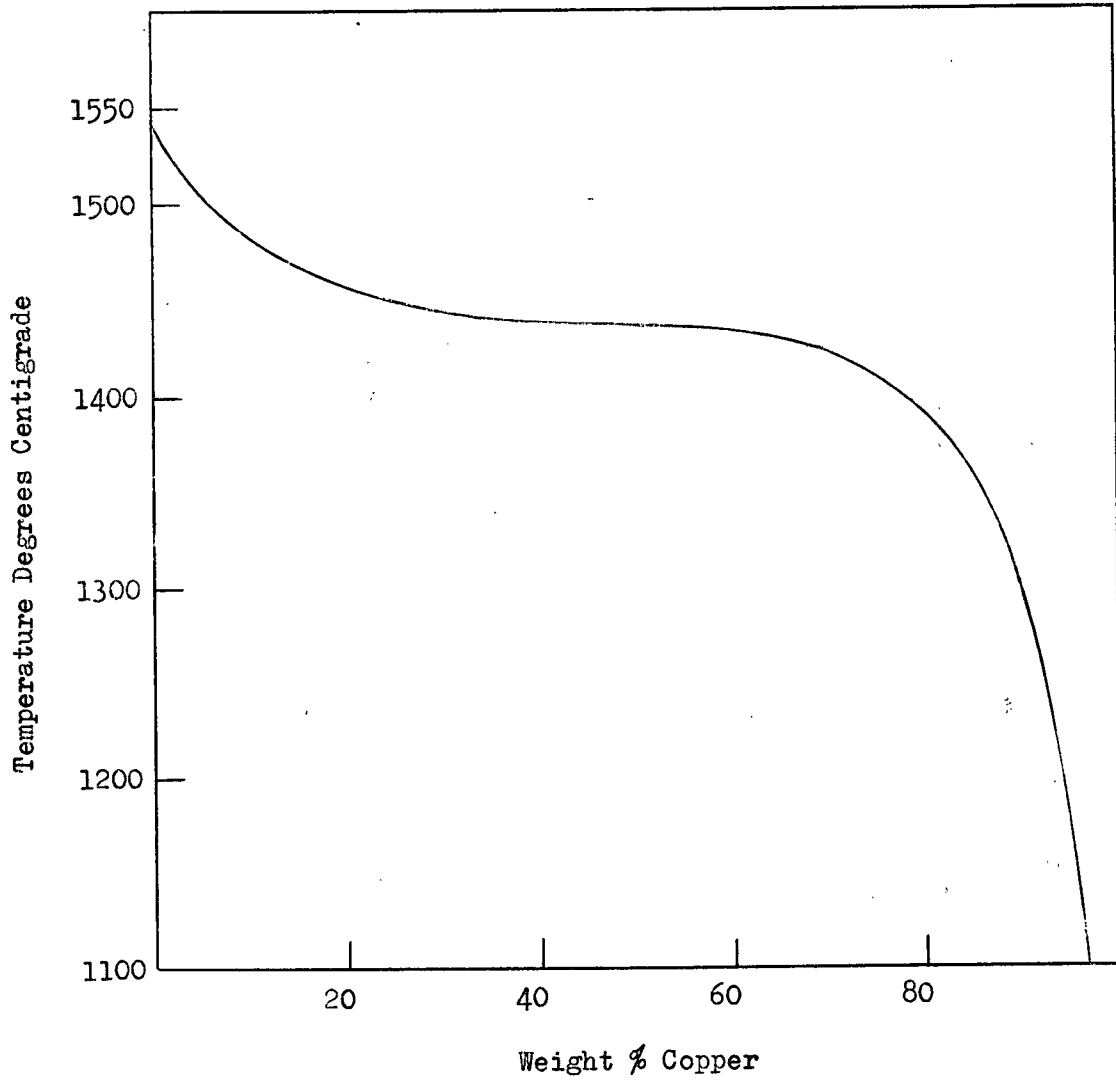


Figure 4. Liquidus Curve, Cu-Fe System¹⁵.

slags containing iron oxide. Prior to the interpretation of experimental results available information on auxiliary systems was examined.

D. Rearrangement of the Equilibrium Constant

The equilibrium constant was rearranged in order to facilitate the calculation of zinc oxide activities from experimental and auxiliary information. This was accomplished by expressing the initial results in the form of a $\frac{\gamma_{ZnO}}{\gamma_{FeO}}$ ratio, i.e.

$$\frac{\gamma_{ZnO}}{\gamma_{FeO}} = K_{1573} \left[\frac{N_{FeO}}{N_{ZnO}} \right] \left[\frac{a_{Zn}}{a_{Fe}} \right]$$

EXPERIMENTAL

A. Materials

Baker and Adamson reagent grade ZnO, CaO, SiO₂, Fe₂O₃, Fe, Cu and Zn materials were used throughout the investigation.

B. Crucibles

The crucibles used were low carbon steel machined from 4" stock (Figure 5). The carbon content was lowered by heating in air at 1300°C for several hours. Several blank runs were made in each crucible before experimental use.

C. Furnace

A simple "Glo Bar" furnace was used (Figure 6). Construction details are shown in Figure 7. The source of power was a 4.5 KVA transformer.

D. Temperature Control

Temperature control was accomplished by means of a Platinum-Rhodium thermocouple attached to a "Wheelco" mercury switch controller. Temperature accuracies were given at $\pm 10^\circ\text{C}$.

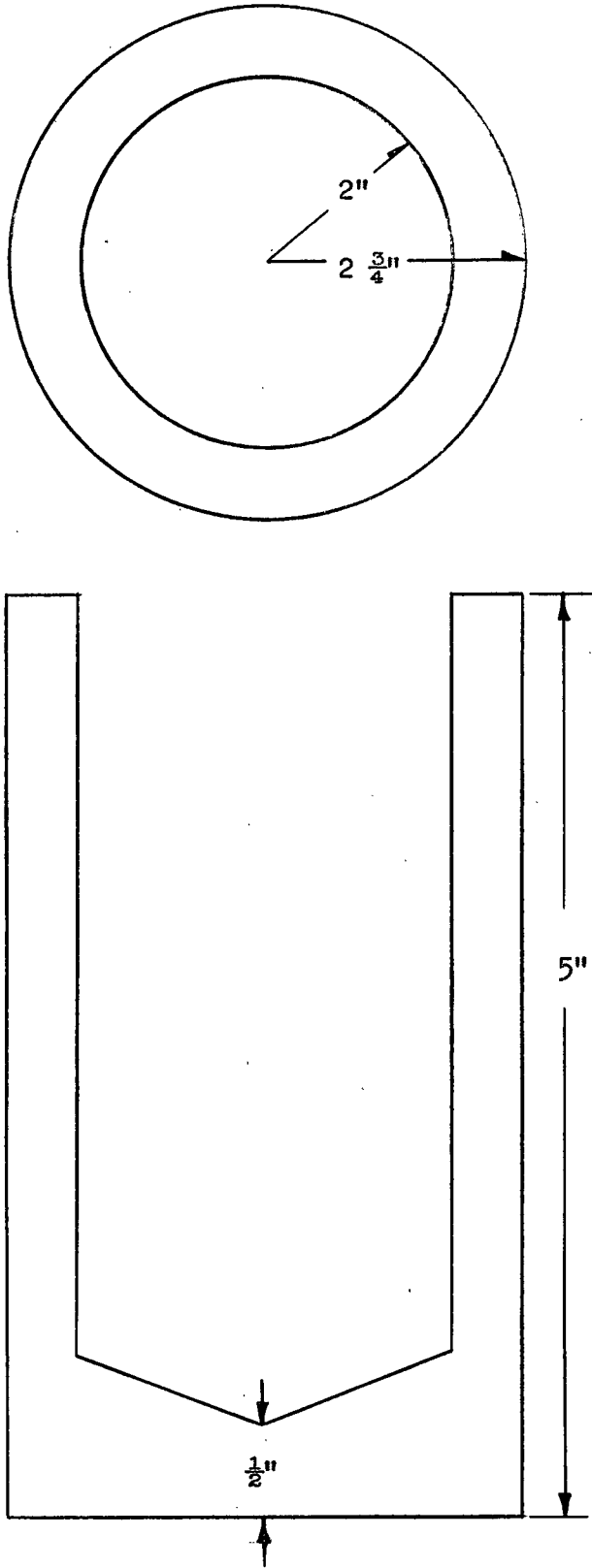


Figure 5. Iron Crucible.

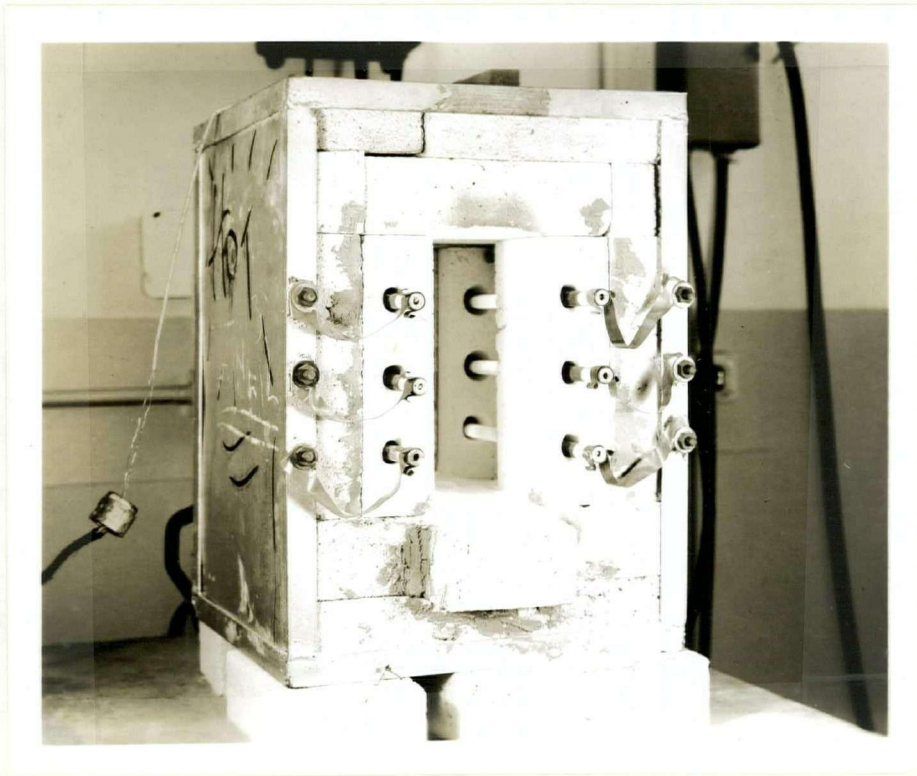
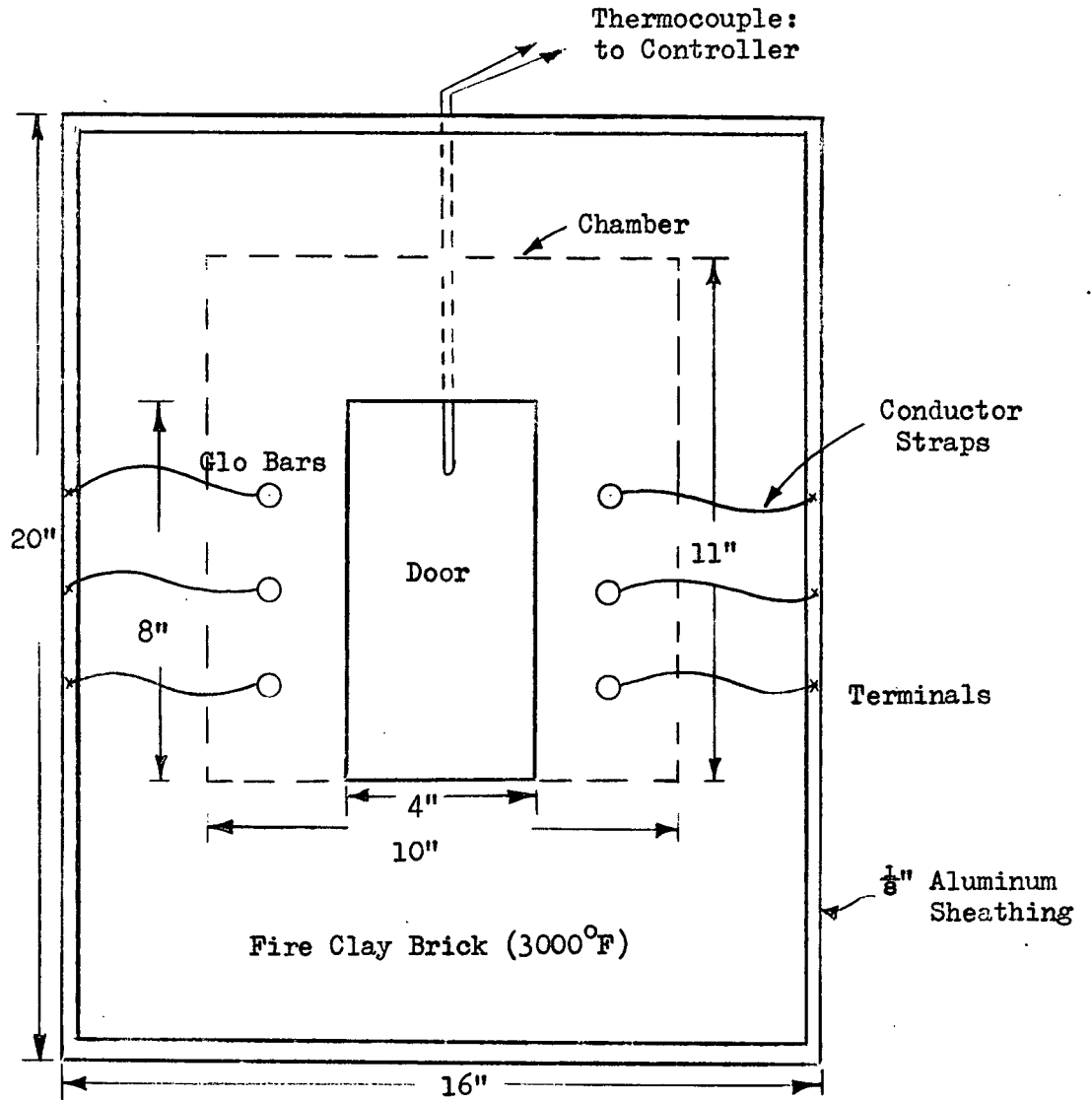


Figure 6. Experimental Furnace



Depth: Furnace 16"
Chamber 10"

Heat Source: 2 sets of 3 "Glo Bars" in parallel

Figure 7. Experimental Furnace, Construction Details.

E. Procedure

Slag and metal components were weighed and mixed. Blending was obtained by passing the mixture through a 35 mesh Tyler screen, followed by remixing. The mixtures were placed in the iron crucible, dried, and charged to the furnace.

Experimental charges consisted of Cu, ZnO, CaO, SiO₂, Fe₂O₃ and Fe powders (Fe and Fe₂O₃ were mixed stoichiometrically to form FeO). During the establishment of equilibrium zinc oxide was reduced by the iron crucible, the resultant zinc entering the metal phase. Several experiments were carried out with an excess of zinc in the metal phase in order to evaluate the effect of the reverse reduction mechanism. The results of the two experimental methods were found to be essentially identical.

Experimental times were between 40 and 70 minutes. Duplicates of each distinct slag type were run at various times, ensuring that equilibrium conditions were attained.

Material balances were calculated in order to eliminate experiments with excessive slag or metal losses. Observed losses were generally in the order of 0 to 3%.

Metal and slag were quenched in iron moulds, thus maintaining equilibrium conditions. Slag-metal separations were also facilitated by using this quenching technique.

F. Assaying

Slag assays were kindly carried out by the Consolidated Mining and Smelting Company of Canada Limited, Trail, B. C. Their assays were reported at $\pm .1\%$.

Metal assays were carried out by Mrs. A. M. Armstrong and the author. Samples were taken by drilling completely through the metal buttons. Copper was determined electrolytically, zinc by potentiometric titration using the potassium ferro-ferricyanide couple, and iron by titration with potassium dichromate. The accuracies of the assays were estimated to be: zinc $\pm 2\%$, iron $\pm 1\%$, Cu $\pm 1\%$.

INVESTIGATION OF THE ZnO-FeO-SiO₂ SYSTEM

The most elementary system which could be studied by the present technique was the ZnO-FeO-SiO₂ system. For this reason an extensive investigation of this system was carried out. Component FeO-SiO₂ and ZnO-SiO₂ systems were examined to provide the required auxiliary information.

A. Auxiliary Systems

1) FeO-SiO₂

The FeO-SiO₂ system has been studied extensively^{16,17,18}. The investigations which give the most consistent results are those of Bodsworth and Davidson¹⁶, and Schuhmann and Ensio¹⁷, who measured the activity of FeO by relations involving oxygen solubility in iron under FeO-SiO₂ slags.

The most recent information on this system is presented in Figures 8 and 9, based on liquid standard states for both FeO and SiO₂. All recent investigations give values in close agreement with this data.

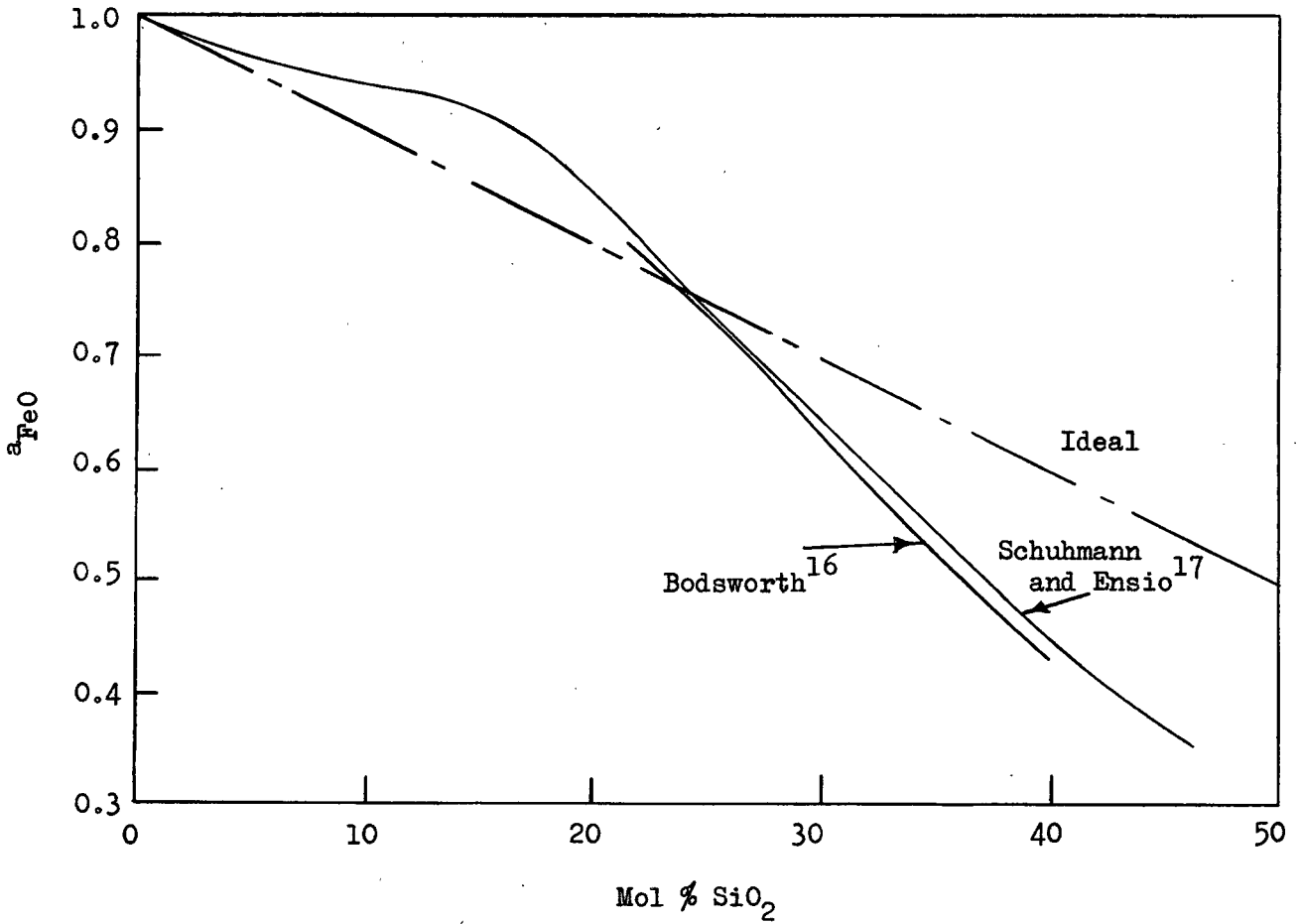


Figure 8. Activity of Ferrous Oxide in Binary Silicate Melts at 1315°C.

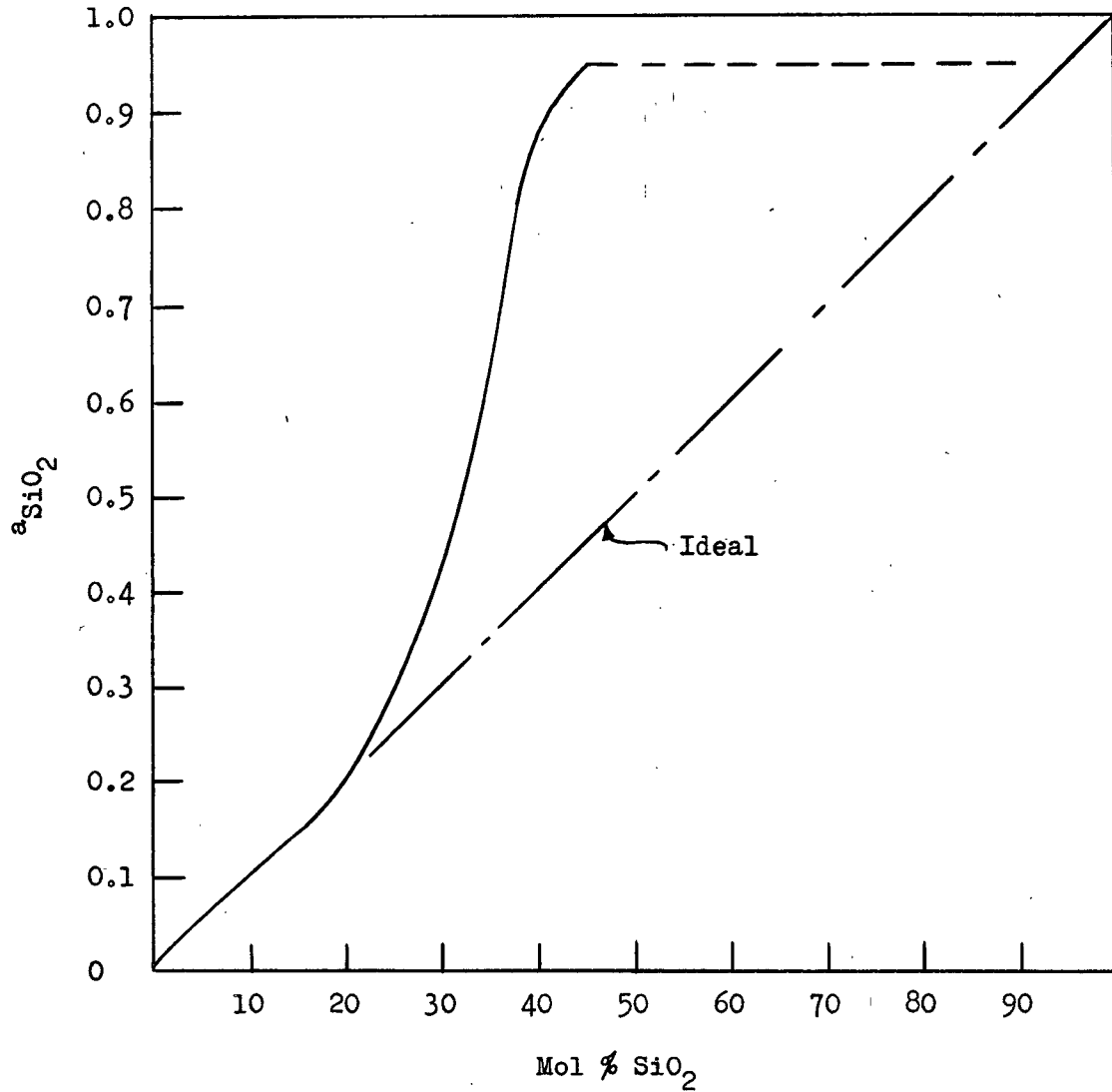
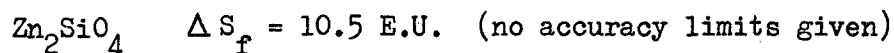
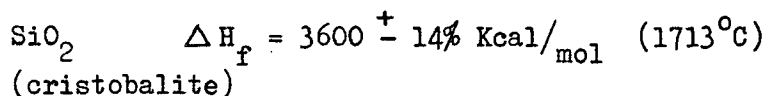


Figure 9. Activity of SiO₂, System FeO-SiO₂, 1300°C
calculated from Schuhmann and Ensio¹⁷.

2) ZnO-SiO₂ System

Because the present experimental technique could not be used to measure activities in the ZnO-SiO₂ system, activities of zinc oxide were calculated from phase diagram and entropy of fusion data.

The phase diagram in the ZnO-SiO₂ system has been investigated¹ (Figure 10). The entropy of fusion of silica¹⁹ and the entropy of fusion of Zn₂SiO₄³ have been estimated.



Using this data the activities of SiO₂ and ZnO were calculated by means of the liquidus curve method of Chipman²⁰ and the congruent melting point method of Hauffe and Wagner²¹ (Appendix II). The results of the activity calculations for this system are shown in Figure 11 and Table 1. (Liquid standard state for both ZnO and SiO₂).

Regular solution plots of FeO and ZnO in their respective silicate systems are shown in Figure 11. These plots provide the best means of interpolating data and also demonstrate the similarities in behaviour patterns in these systems.

A regular solution plot of CaO-SiO₂ activity data^{22,23} is included to show the relative position of zinc oxide activities in binary silicate systems.

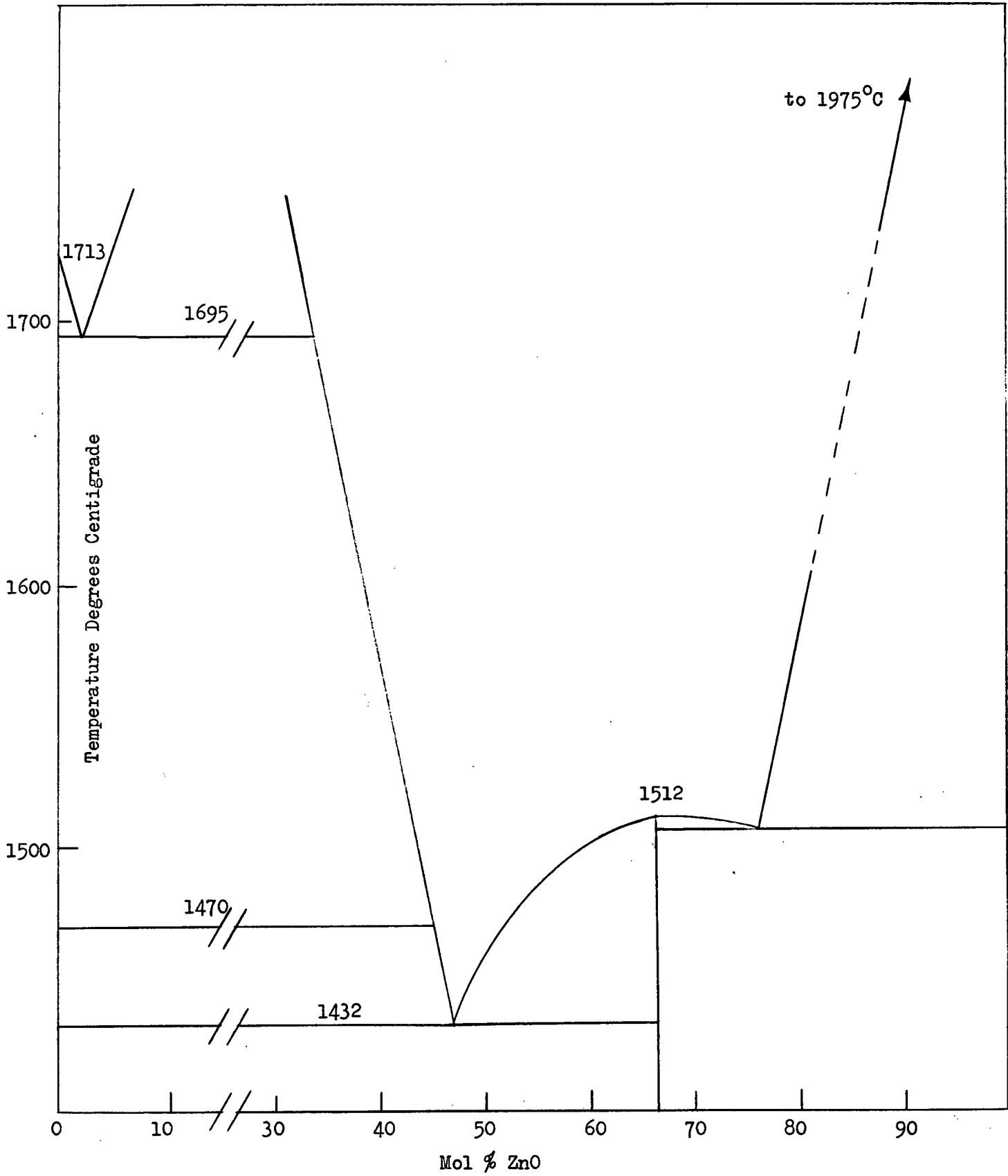


Figure 10. Phase Diagram, ZnO-SiO₂ System¹.

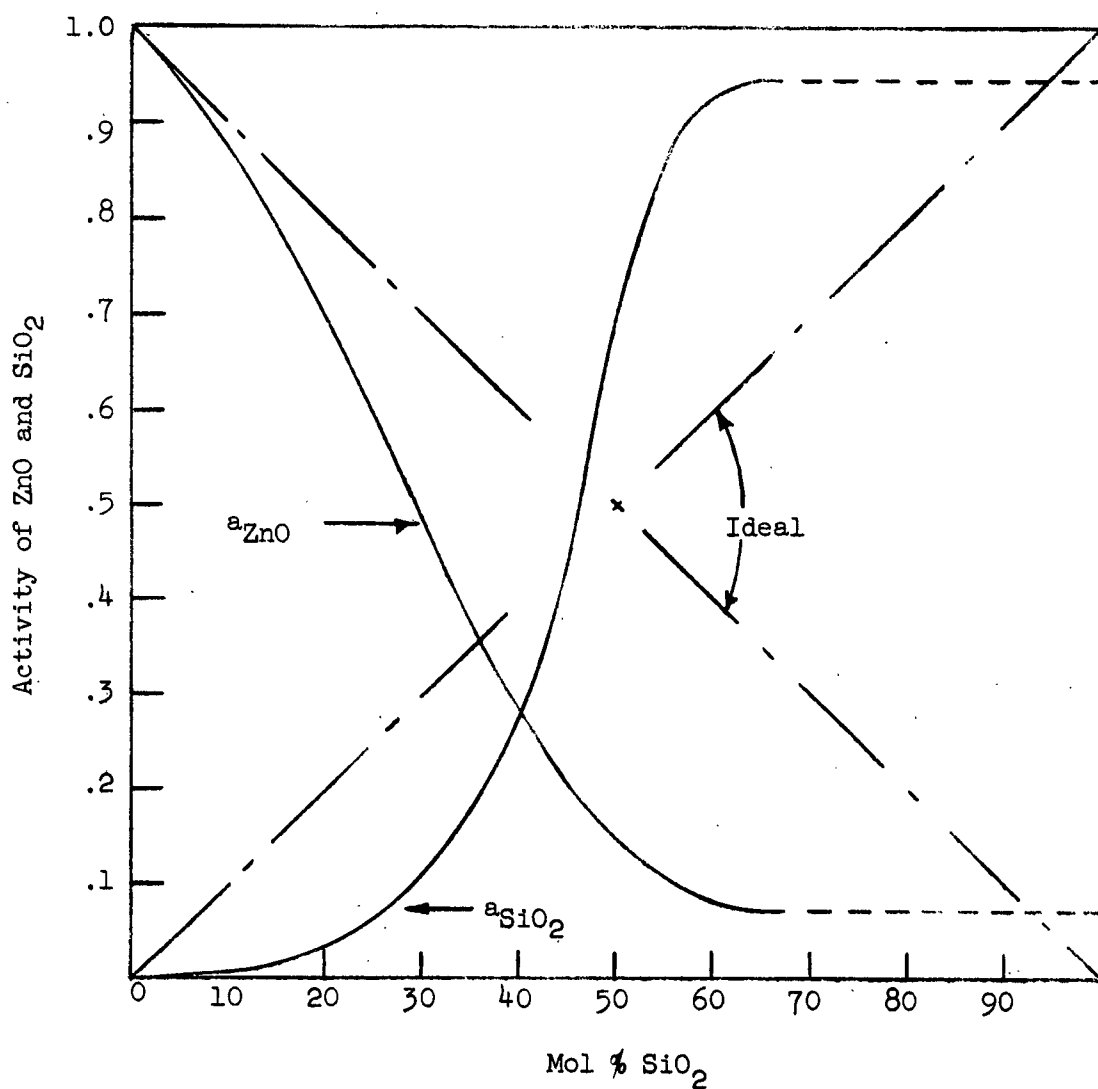


Figure 11. The Activities of ZnO and SiO₂, ZnO-SiO₂ System, 1300°C.

Table 1.

Activities of ZnO and SiO₂, ZnO-SiO₂ System, 1300°C.

N_{SiO_2}	a_{ZnO}	a_{SiO_2}	N_{ZnO}
0	1	0	1
.1	.87	.008	.9
.2	.70	.029	.8
.3	.47	.11	.7
.4	.26	.295	.6
.5	.13	.70	.5
.6	.08	.946	.4
.7	.073	.946	.3
.8	.073	.946	.2
.9	.073	.946	.1
1	0	1	0

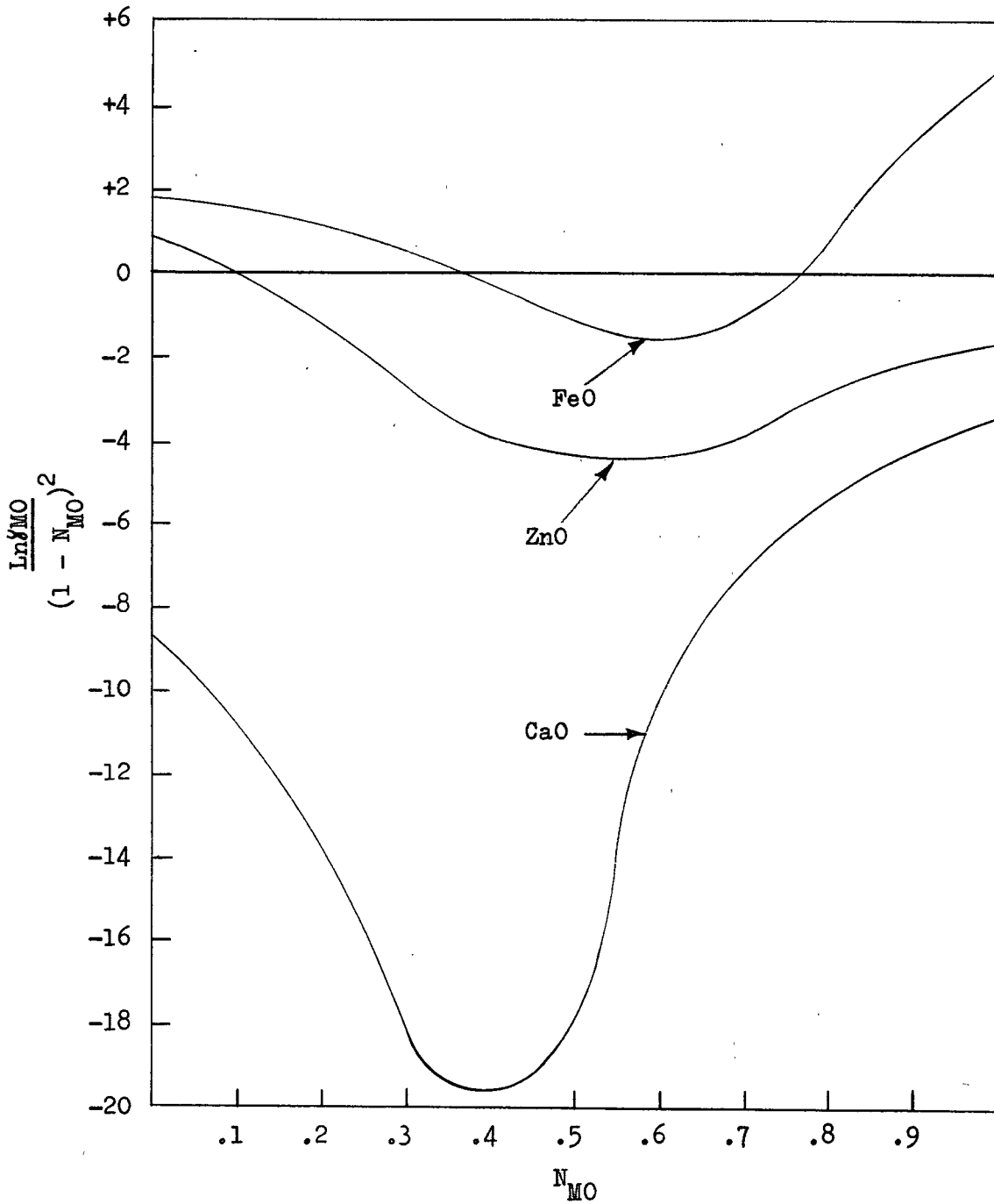


Figure 12. Regular Solution Plots of ZnO, FeO, and CaO in Binary Silicate Systems, 1600°C.

3) Silica Activities, ZnO-FeO-SiO₂ System

The silica isoactivity pattern in the ZnO-FeO-SiO₂ system was obtained from the above ZnO-SiO₂ and FeO-SiO₂ information. Iso-silicate lines were obtained by joining points of identical silica activity on the two binaries.

No phase diagram information on the ZnO-FeO-SiO₂ system was available to establish the curvature of the silica isoactivity lines. Curvatures consistent with observed isoactivity patterns of similar systems (ZnO-CaO-SiO₂, Figure 27; FeO-CaO-SiO₂, Figure 22) were assigned (Figure 13).

B. Experimental Zinc Oxide Activity Determination, System ZnO-FeO-SiO₂

Experiments on the ZnO-FeO-SiO₂ system were carried out at three silica concentration levels. Zinc oxide and iron oxide compositions were varied at each level.

The experimental $\gamma_{\text{ZnO}}/\gamma_{\text{FeO}}$ ratios were calculated from measured a_{Zn} values. The results are shown in Figure 14 and Appendix III. The $\gamma_{\text{ZnO}}/\gamma_{\text{FeO}}$ ratios were found to vary linearly with ZnO concentration at each silica level. Comparisons with other slag systems (ZnO-CaO-SiO₂, FeO-CaO-SiO₂) showed that this linear variation was to be expected.

A technique of approximations was developed in order to evaluate ZnO activities from experimental $\gamma_{\text{ZnO}}/\gamma_{\text{FeO}}$ ratios. Two approximation steps were employed.

1) First Approximation, Zinc Oxide Activity Calculation

The calculation of zinc oxide activity was initiated by first

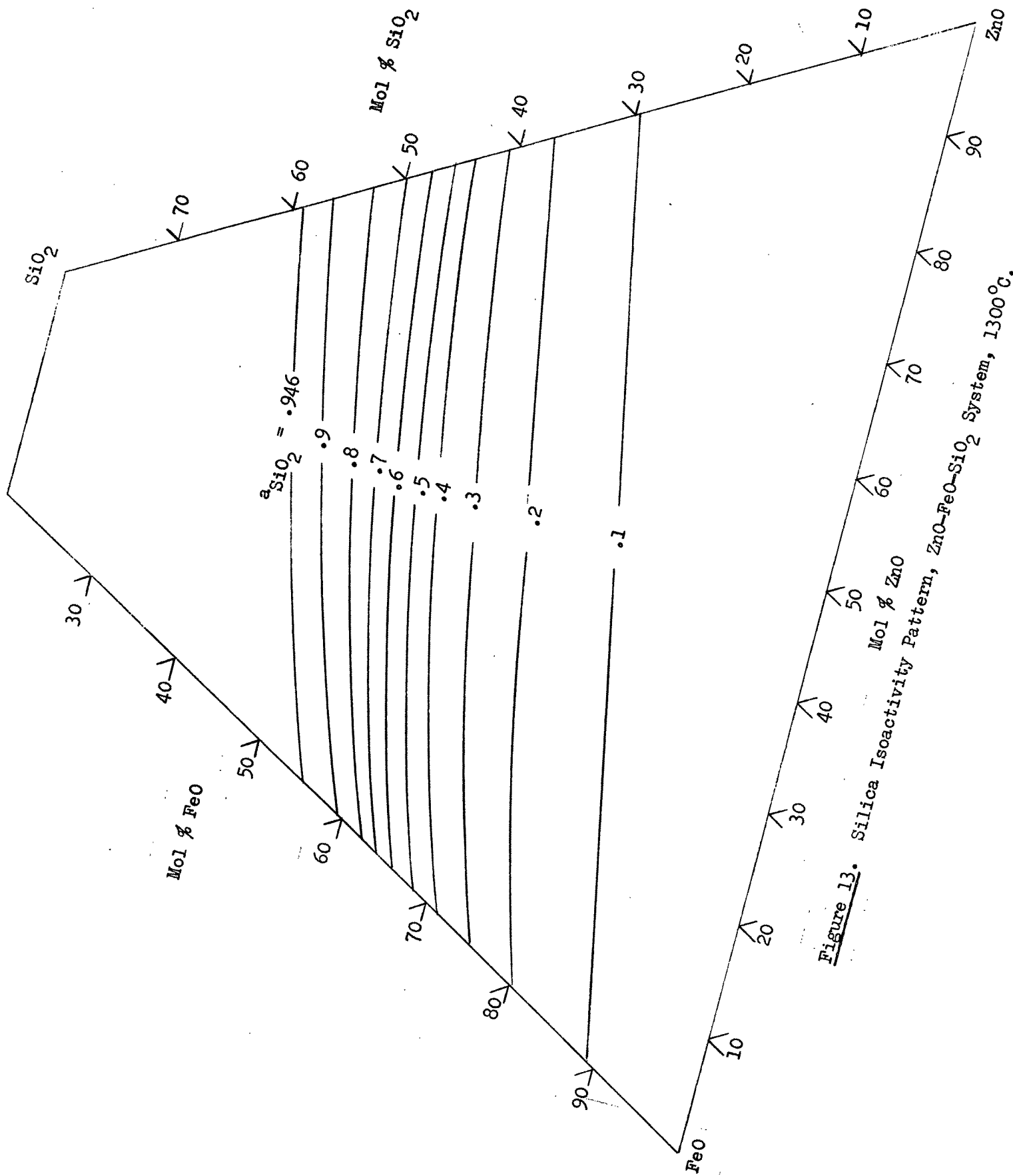


Figure 13. Silica Isoactivity Pattern, ZnO-FeO-SiO₂ System, 1300°C.

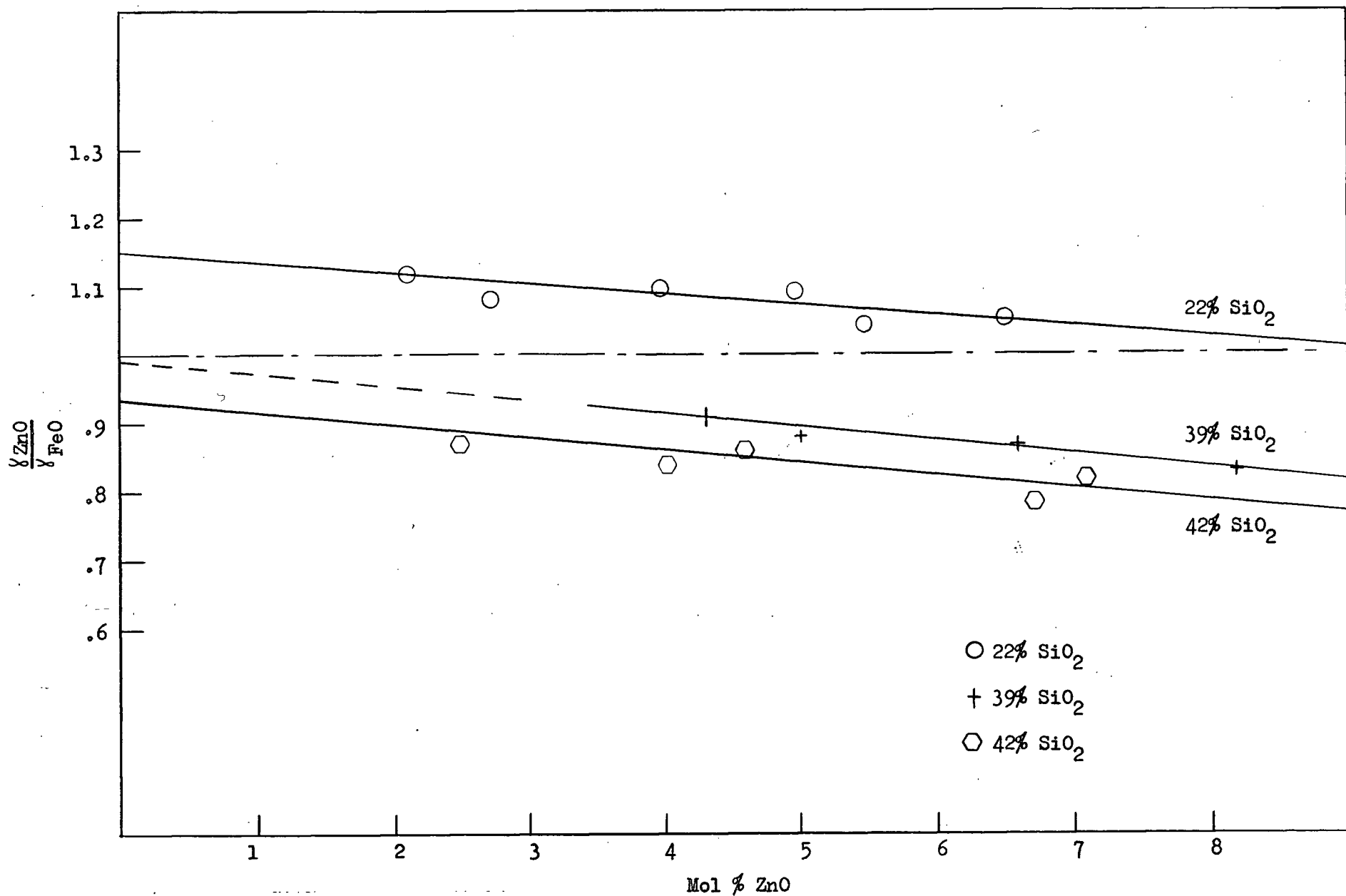


Figure 14. Experimental Activity Coefficient Ratios, ZnO-FeO-SiO₂ System, 1300°C.

making the assumption that iron oxide activity is constant at constant silica concentration over the experimental range. Iron oxide activity values were evaluated from the binary FeO-SiO₂ system (Figure 8) and were projected along the silica concentration lines. The FeO activity coefficients were then evaluated for the experimental ZnO concentrations. These activity coefficients were applied to the experimentally determined coefficient ratios, giving approximate ZnO activity values. Points of identical activity were then joined, creating tentative ZnO isoactivity lines.

2) Final Determination of a_{ZnO}

From the tentative ZnO isoactivity model precise values of a_{ZnO} were evaluated. Using available silica isoactivity lines (Figure 13), more accurate γ_{FeO} values were obtained by thermodynamic analysis of the system. (The three methods employed are outlined on page 7.) Zinc oxide activities were then recalculated on the basis of the re-evaluated γ_{FeO} data.

The technique of successive approximations produced mutually consistent activity values for FeO and ZnO and created a thermodynamically rigid isoactivity pattern over the experimental range. The results are shown in Figures 15 and 15a and Appendix III.

C. Accuracy of Experimental Zinc Oxide Activities

The accuracy of the experimental zinc oxide activities was estimated to be $\pm 43\%$.

The possible errors involved in the use of the equilibrium constant ($\pm 15\%$) and zinc activities in the Zn-Cu-Fe system ($\pm 16\%$) have been discussed (Schuhmann and Ensio¹⁷ report their a_{FeO} values are accurate to within $\pm 2\%$).

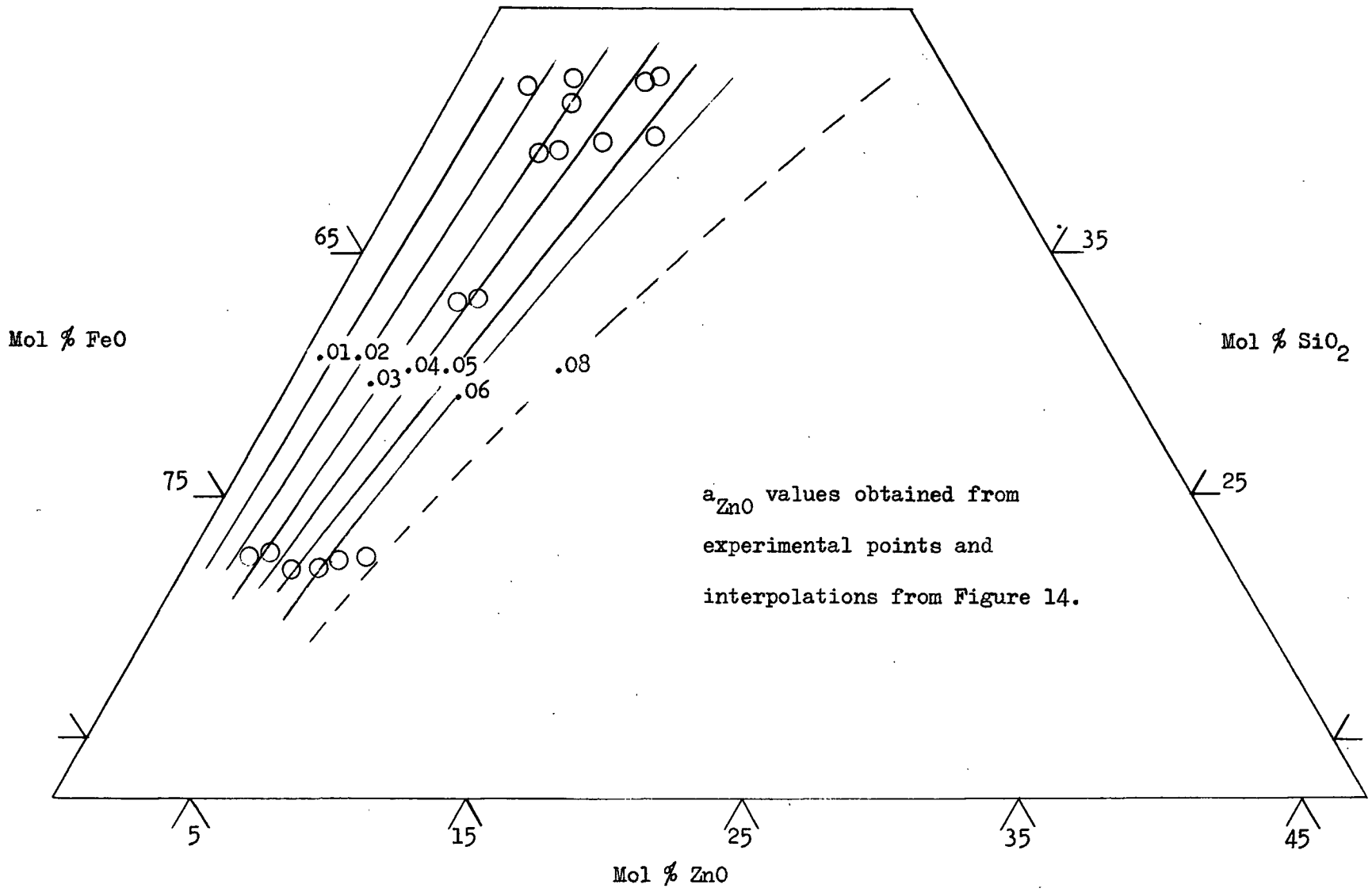


Figure 15. Experimental Zinc Oxide Isoactivity Lines, ZnO-FeO-SiO₂ System, 1300°C.

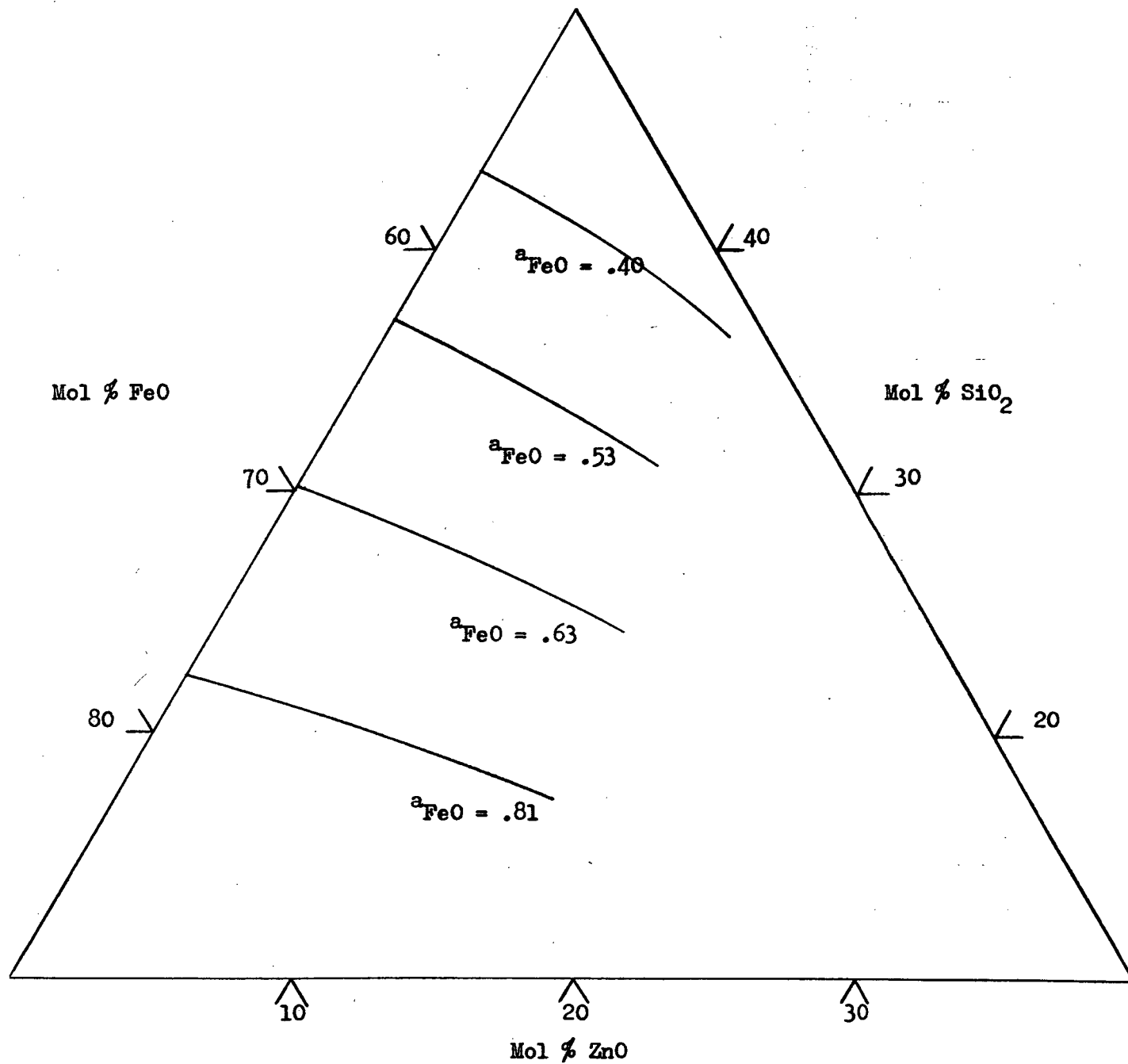


Figure 15a. Iron Oxide Isoactivity Pattern, ZnO-FeO-SiO₂ System, 1300°C.
 Developed during calculation of a_{ZnO} .

The errors in the approximation techniques were estimated to be $\pm 10\%$. This estimate was made on the basis of activity variations detectable in the application of the Gibbs Duhem equation to the experimental values.

D. Summary of Thermodynamic Data, ZnO-FeO-SiO₂ System

A comprehensive thermodynamic treatment of the ZnO-FeO-SiO₂ system was obtained from the experimental results.

Extensions of the experimental data were obtained by a thermodynamic analysis of the system (Appendix IV). The auxiliary FeO-SiO₂ and ZnO-SiO₂ systems were also consulted.

Because considerable slag information is reported at 1600°C, the experimental data was extrapolated to this temperature using the regular solution model. Rey²⁴ has pointed out that this model is applicable over large ranges of silicate systems.

One assumption was made during the calculations. The $\gamma_{\text{ZnO}}/\gamma_{\text{FeO}}$ ratio data at 41% SiO₂ was extrapolated linearly to 15% ZnO. This assumption made possible the extension of the $a_{\text{ZnO}} = .1$ isoactivity line to the ZnO-SiO₂ binary, thus facilitating the analysis of the system.

The results of the calculations are shown in Figures 16, 17 and 18.

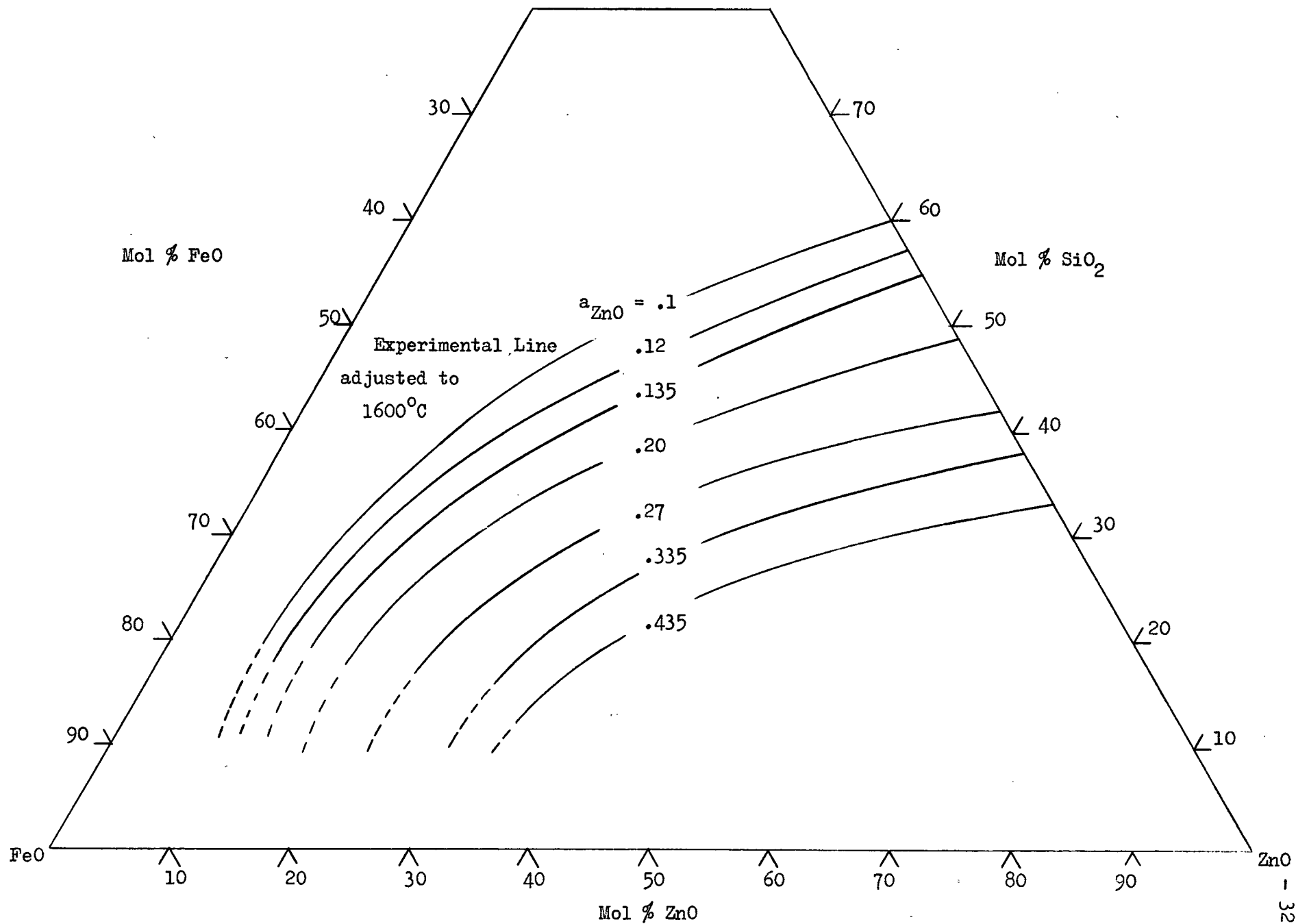


Figure 16. Summary of Zinc Oxide Activity Data, ZnO-FeO-SiO₂ System, 1600°C.

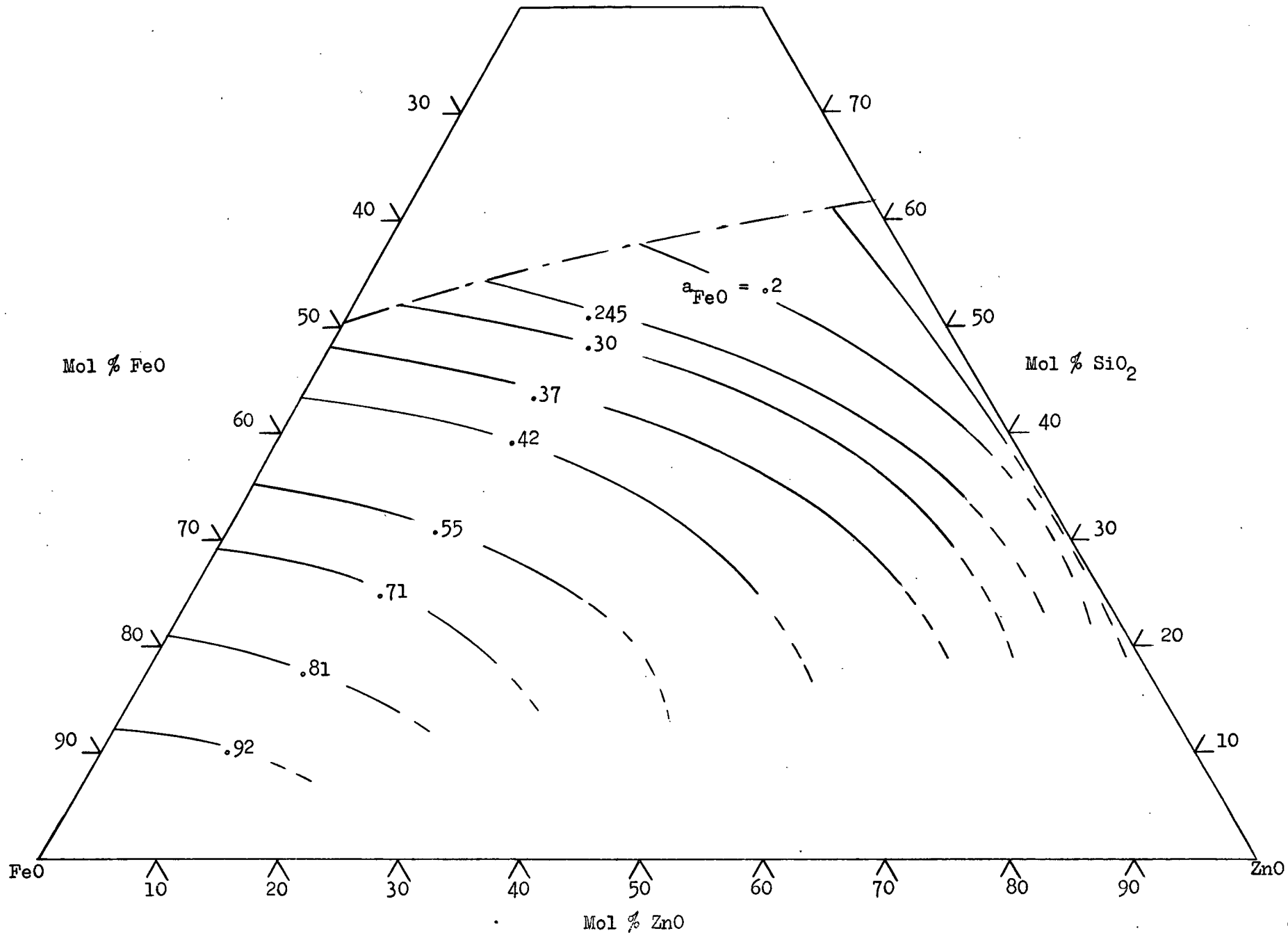


Figure 17. Summary of Iron Oxide Activity Data, ZnO-FeO-SiO₂ System, 1600°C.

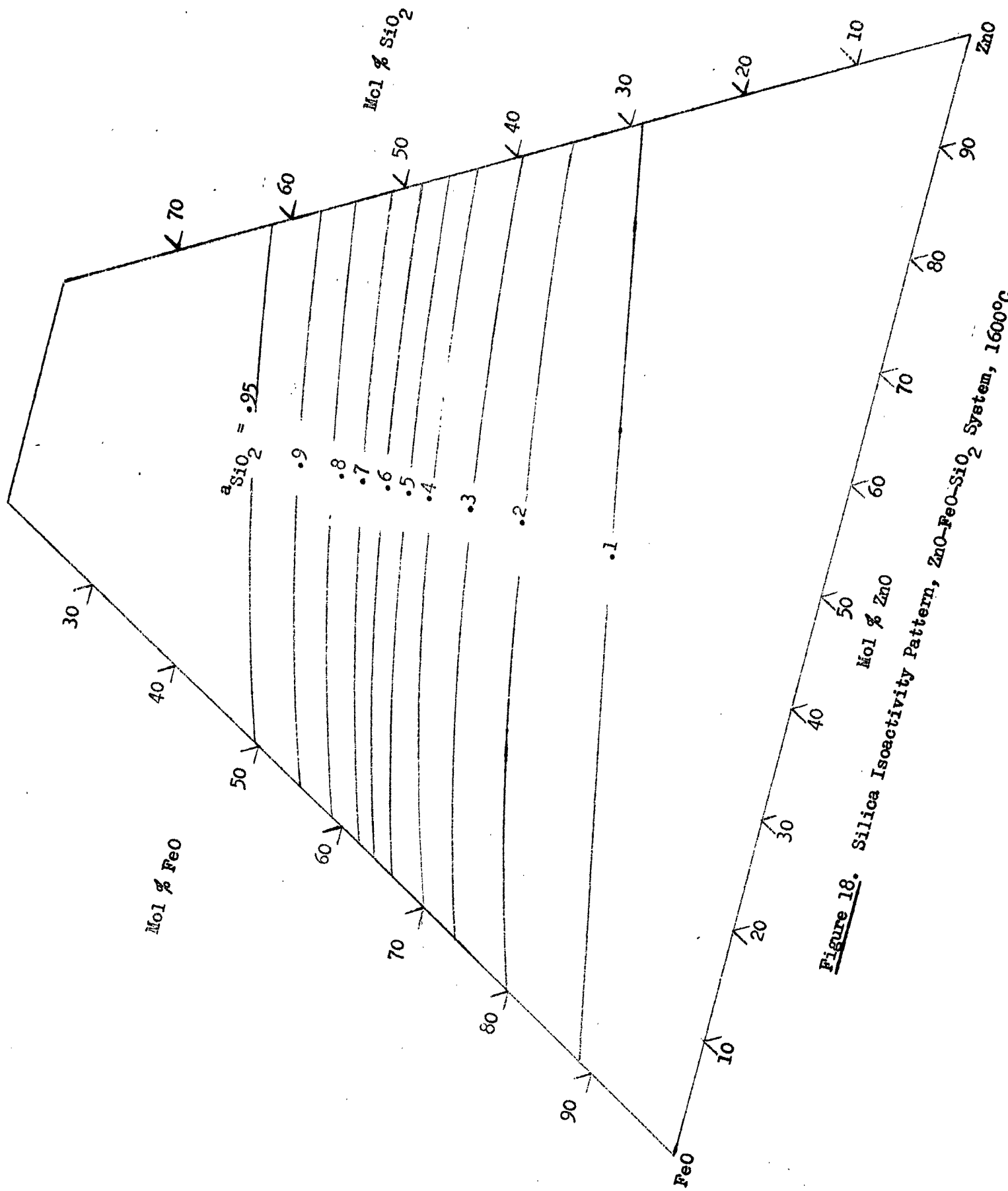


Figure 18. Silica Isoactivity Pattern, ZnO-FeO-SiO₂ System, 1600°C.

INVESTIGATION OF THE ZnO-FeO-CaO-SiO₂ SYSTEM

Because the ZnO-FeO-CaO-SiO₂ system closely approximates the compositions of industrial slags, an extensive investigation of this system was made. Zinc oxide activities were measured over extensive ranges of silica, lime, and iron oxide compositions.

Examinations of the component ternary systems were made to provide the auxiliary information required for the determination of zinc oxide activities. The ternary systems examined were the ZnO-FeO-SiO₂, FeO-CaO-SiO₂ and ZnO-CaO-SiO₂ systems.

A. Auxiliary Systems

1) ZnO-FeO-SiO₂ System

The activities in the ZnO-FeO-SiO₂ system were evaluated and summarized earlier in the investigation (Figures 16, 17 and 18).

2) FeO-CaO-SiO₂ System

The FeO-CaO-SiO₂ system has been studied extensively by Winkler and Chipman²⁵, Taylor and Chipman²⁶, Turkdogan and Pearson²⁷, and others. Elliot²⁸ has made a comprehensive review of these studies and, by application of the Gibbs Duhem equation, has determined activities of all components in the system. The slags investigated contained small amounts of MgO, but according to Elliot, the similar behaviour of CaO and MgO allows the results to be interpreted as activities in the simple FeO-CaO-SiO₂ ternary system.

More recent information on the CaO-SiO_2 system^{22,23} (Figure 19 and Table 2) was applied to the FeO-CaO-SiO_2 system and Elliot's results were re-evaluated in co-operation with G. W. Toop²⁹. The re-evaluated activity pattern is shown in Figures 20, 21 and 22.

3) ZnO-CaO-SiO_2 System

At the outset of the investigation, it was hoped that the activity of ZnO in the ZnO-CaO-SiO_2 system could be measured by a slag metal equilibrium technique.

Two main difficulties were encountered. Firstly, slag melting points were prohibitive over the low ZnO range of compositions. Secondly, no satisfactory equilibrium reactions could be established. For these reasons, the system was analyzed thermodynamically by the methods outlined on page 7.

The data used in the calculation of activities were:

- i) Zinc oxide and silica activities in the ZnO-SiO_2 system (Figure 23).
- ii) Lime and silica activities in the CaO-SiO_2 system^{22,23} (Figure 19).
- iii) Lime, silica and zinc oxide saturation lines in the ZnO-CaO-SiO_2 system² (Figure 24).

The ZnO-CaO-SiO_2 system was analyzed thermodynamically on the basis of this data and a rigid isoactivity pattern was developed (Figures 25, 26 and 27).

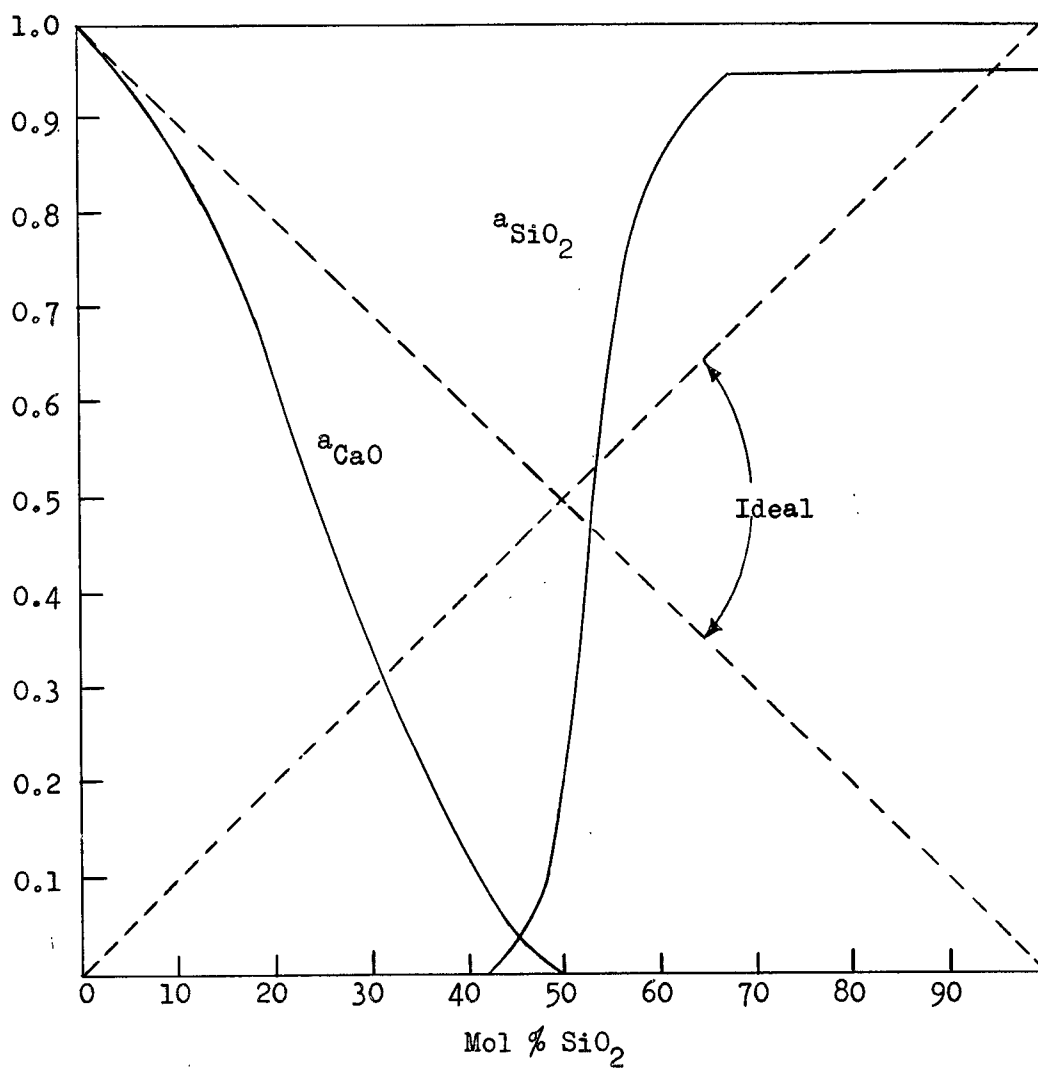


Figure 19. Activities in the CaO-SiO₂ System, 1600°C^{22,23}.

Table 2.

Activities in the CaO-SiO₂ System, 1600°C.

N_{SiO_2}	a_{CaO}	a_{SiO_2}	N_{CaO}
.07	.92	.000015	.93
.18	.69	.000105	.82
.26	.48	.00038	.74
.33	.28	.0013	.67
.39	.14	.005	.61
.45	.04	.03	.55
.48	.013	.10	.52
.49	.0068	.20	.51
.52	.0031	.40	.48
.54	.0021	.60	.46
.58	.0012	.80	.42
.62	.0005	.90	.38
.67	.00005	.95	.33

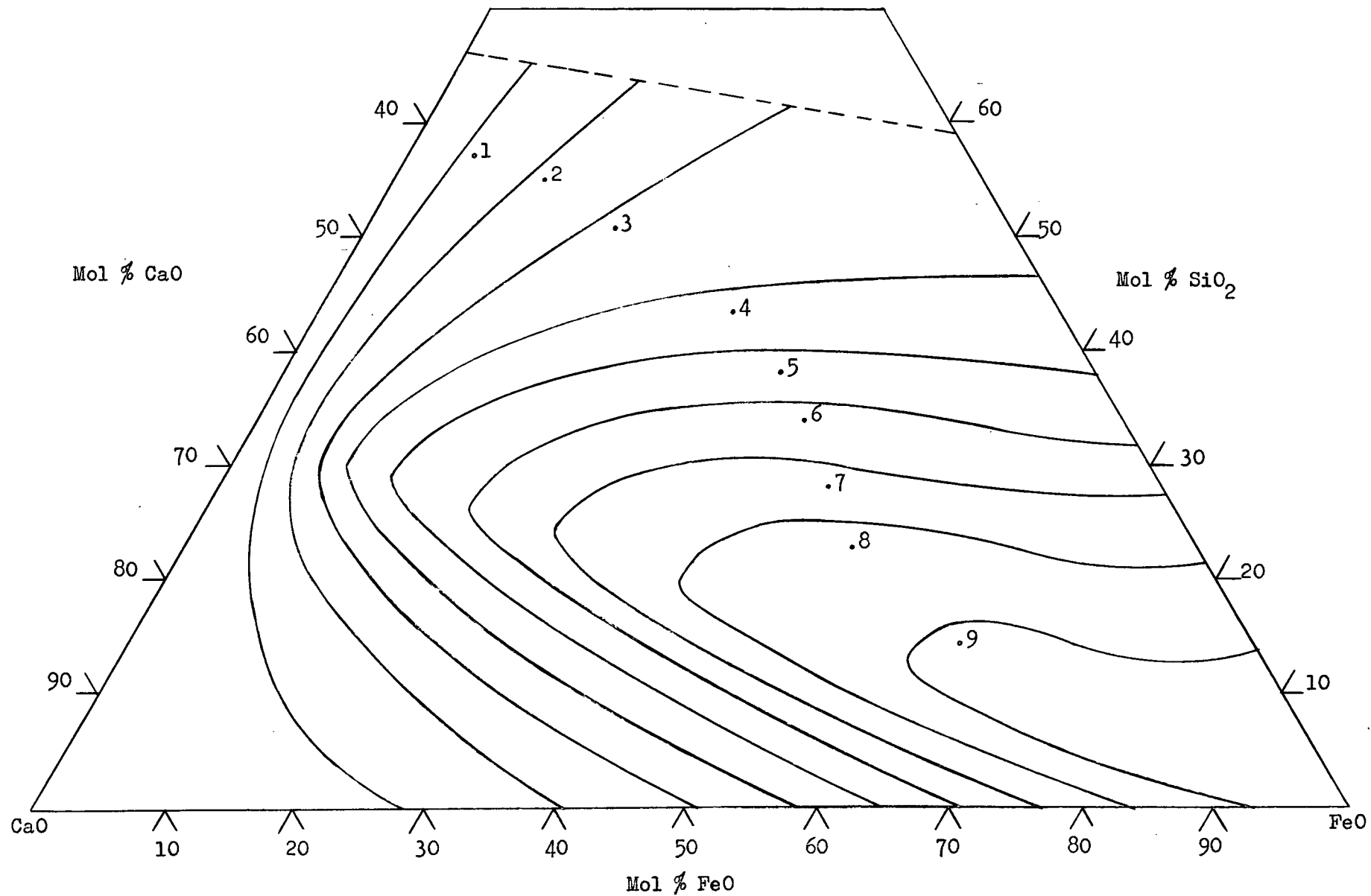


Figure 20. Iron Oxide Isoactivity Pattern, FeO-CaO-SiO₂ System, 1600°C.²⁸

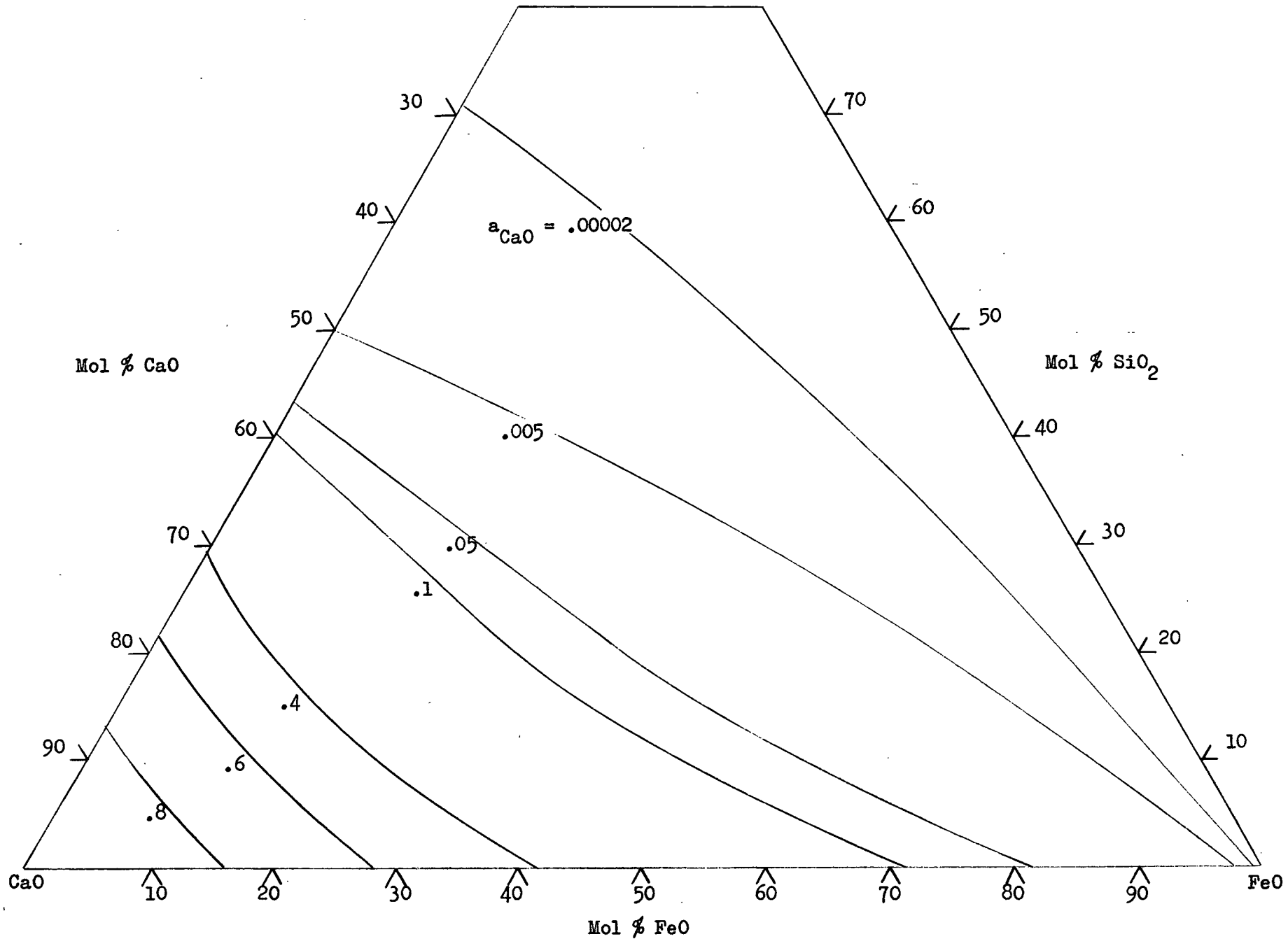


Figure 21. CaO Isoactivity Pattern, FeO-CaO-SiO₂ System, 1600°C.

From the data of Elliot²⁸.

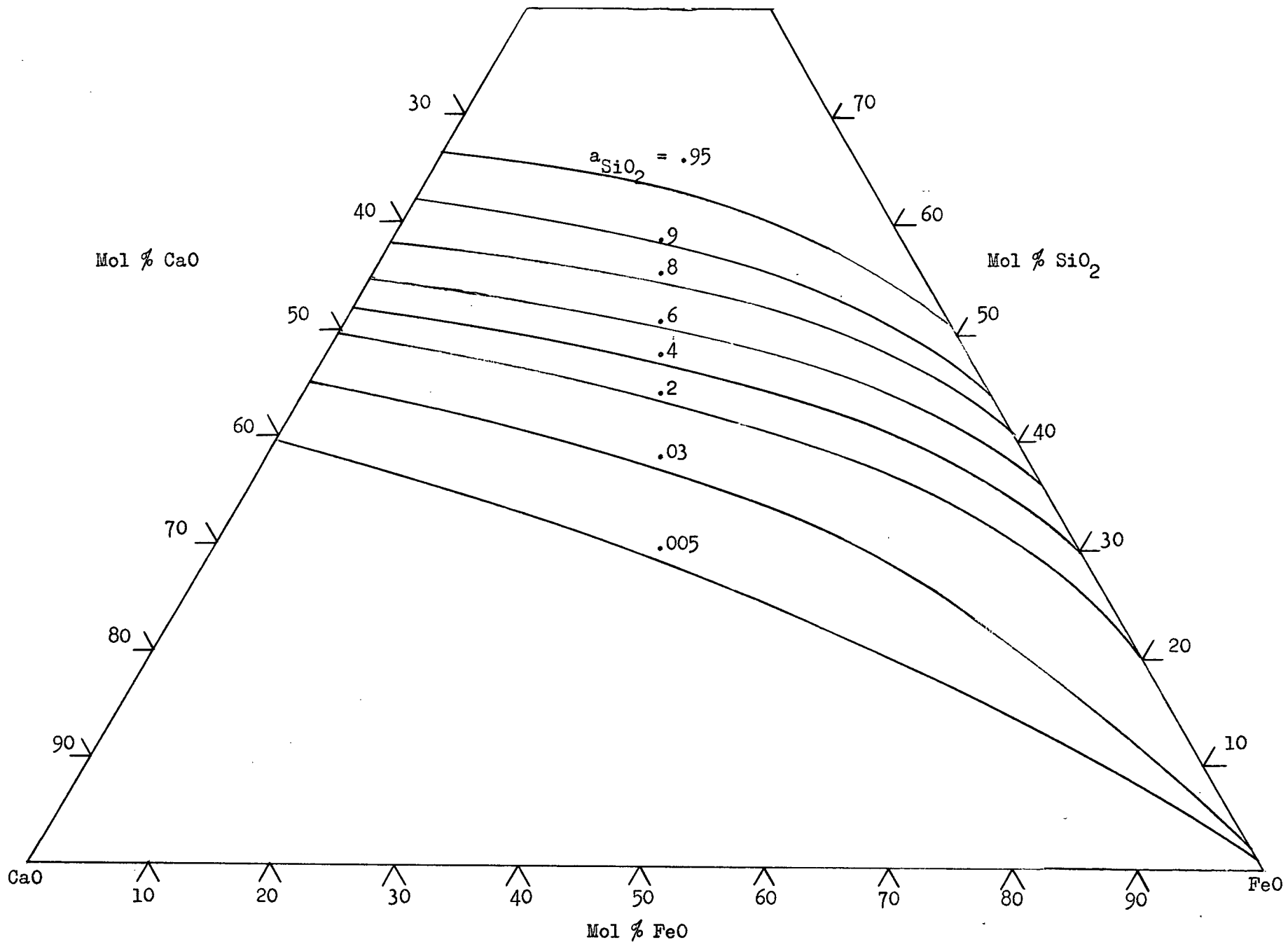


Figure 22. Silica Isoactivity Pattern, FeO-CaO-SiO₂ System, 1600°C.²⁸

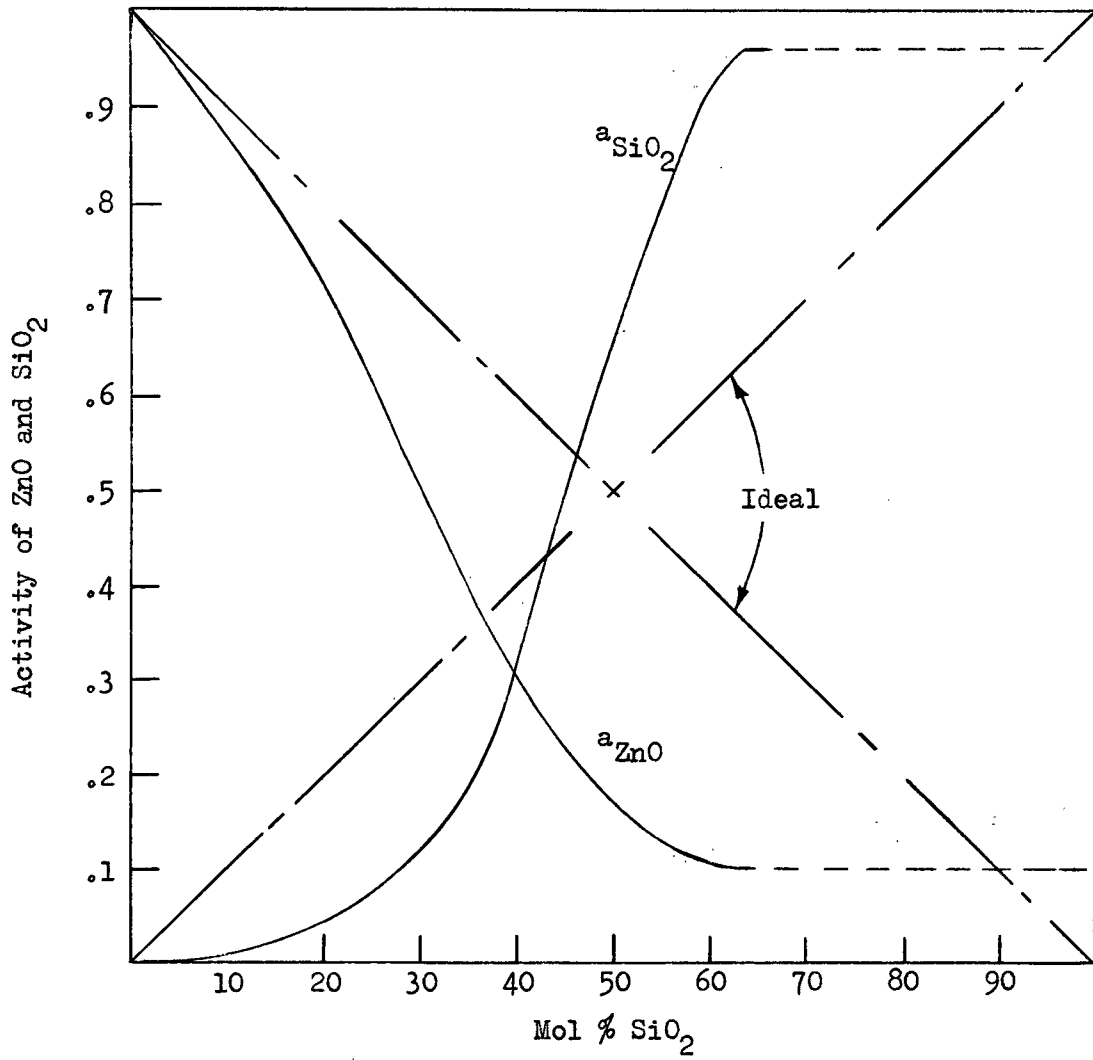


Figure 23. Activities of ZnO and SiO₂, ZnO-SiO₂ System, 1600°C.

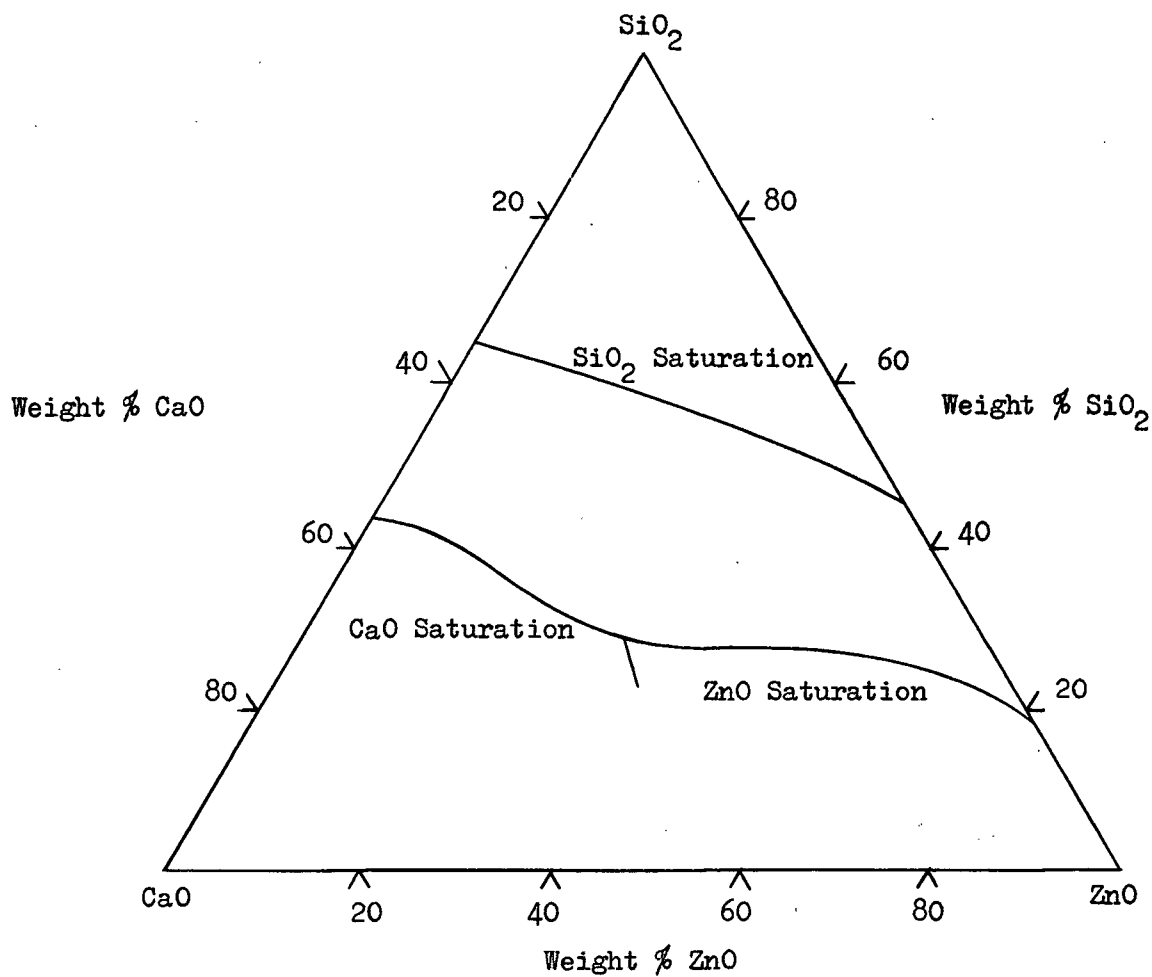


Figure 24. Phase Diagram, ZnO-CaO-SiO₂ System Showing Shapes of Saturation Lines at 1500°C.

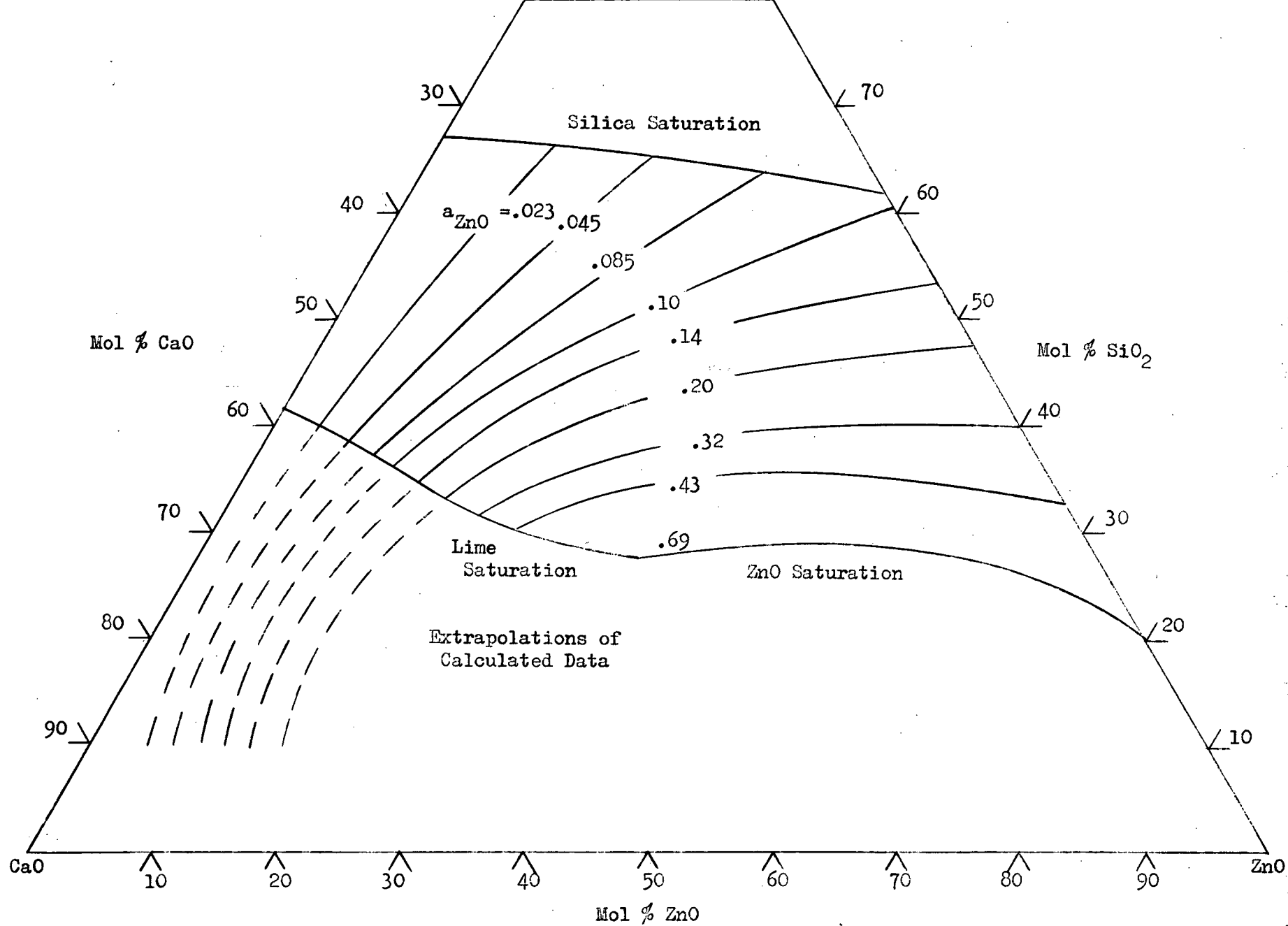


Figure 25. Zinc Oxide Isoactivity Pattern, System ZnO-CaO-SiO₂, 1600°C.

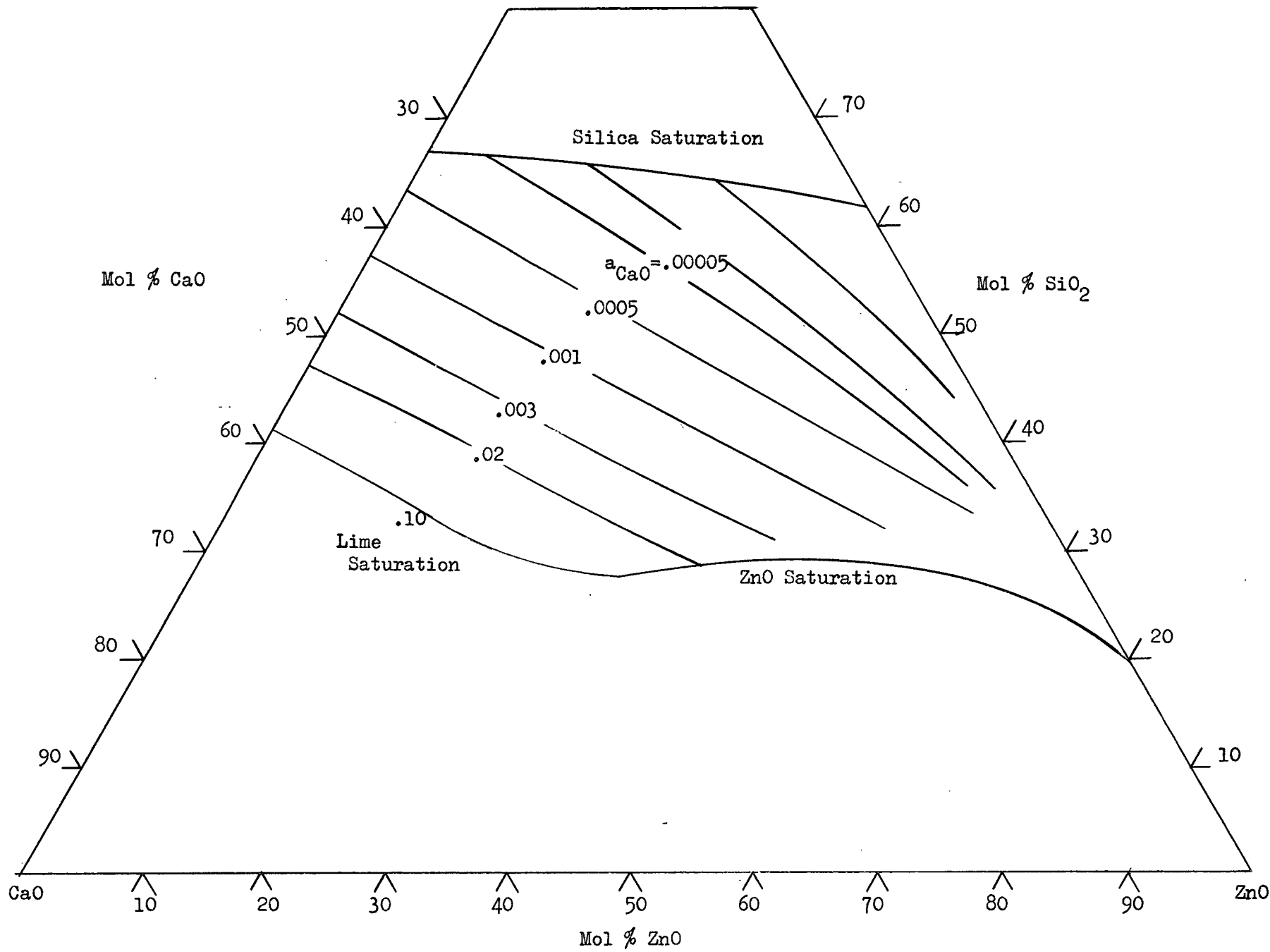


Figure 26. Lime Isoactivity Pattern, ZnO-CaO-SiO₂ System, 1600°C.

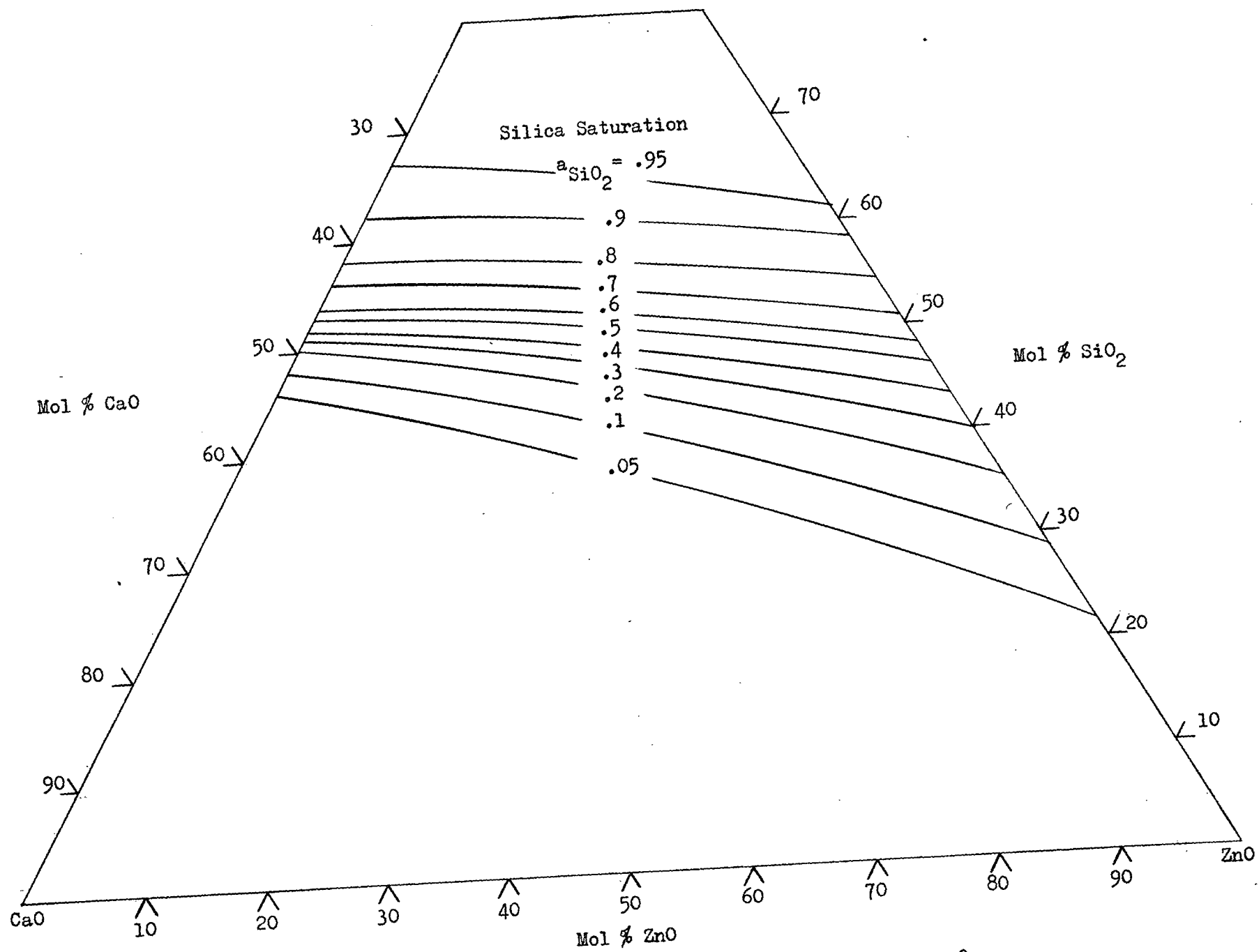


Figure 27. Silica Isoactivity Pattern ZnO-CaO-SiO₂ System, 1600°C.

B. Experimental Zinc Oxide Activity Determination, System ZnO-FeO-CaO-SiO₂

Experimental measurements on the ZnO-FeO-CaO-SiO₂ system were carried out at five silica concentration levels, the CaO, FeO, and ZnO concentrations being varied at each level. The experimental $\frac{\gamma_{\text{ZnO}}}{\gamma_{\text{FeO}}}$ ratios at each silica level are tabulated in Appendix VI.

Zinc activities were interpreted by effectively 'slicing' the quaternary system at each experimental silica level. Each 'slice' then represented a 'pseudo-ternary' cut.

On each cut the intercepts of the FeO and ZnO isoactivity lines were known from evaluations of the ZnO-CaO-SiO₂, ZnO-FeO-SiO₂, and FeO-CaO-SiO₂ systems.

It was found that on both the ZnO-FeO-SiO₂ and FeO-CaO-SiO₂ systems the iron oxide isoactivity lines were nearly parallel to the silica slices. This meant that on the 'pseudo-ternary' cuts FeO activities appeared as planes of almost constant activity over the experimental regions.

This activity behaviour of FeO simplified the determination of a_{ZnO} . FeO activities could be assigned with good accuracy over the experimental region on each cut, and a_{ZnO} could be evaluated from the experimental activity coefficient ratios. It was estimated that the use of this calculation technique in the determination of zinc oxide activities introduced possible errors of $\pm 10\%$. These limits were based on a_{FeO} accuracy limits in the FeO-CaO-SiO₂ and ZnO-FeO-SiO₂ systems and possible a_{FeO} variations on the 'pseudo-ternary' cuts.

Zinc oxide activities were calculated (Appendix VI) and plotted at each experimental point, and isoactivity lines were drawn including the intercepts on the ZnO-FeO-SiO₂ and ZnO-CaO-SiO₂ systems. The results are shown in Figures 28, 29, 30 and 31.

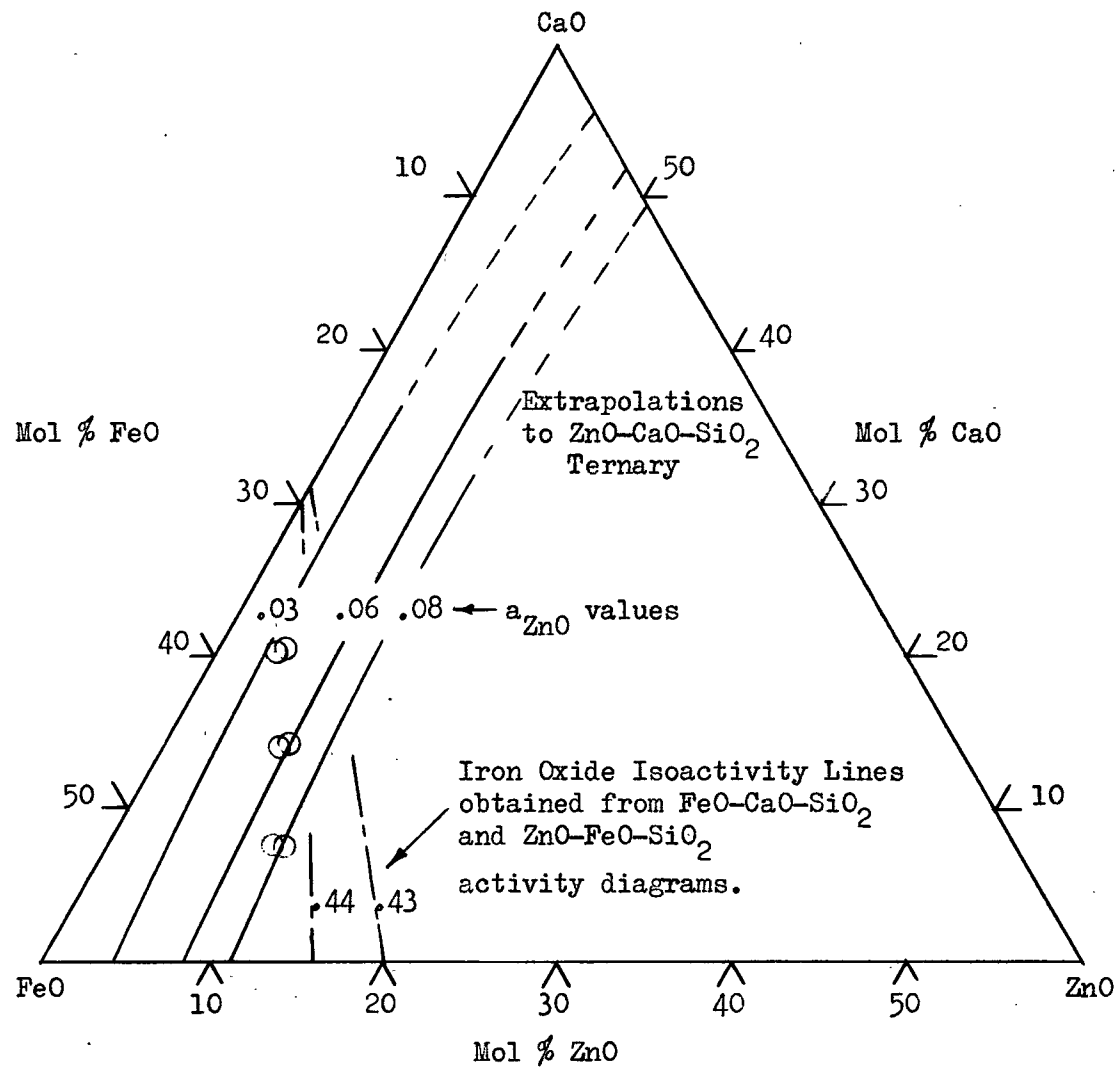


Figure 28. Isoactivity Patterns, ZnO-FeO-CaO-SiO₂ System, 1600°C.
40% SiO₂ Cut

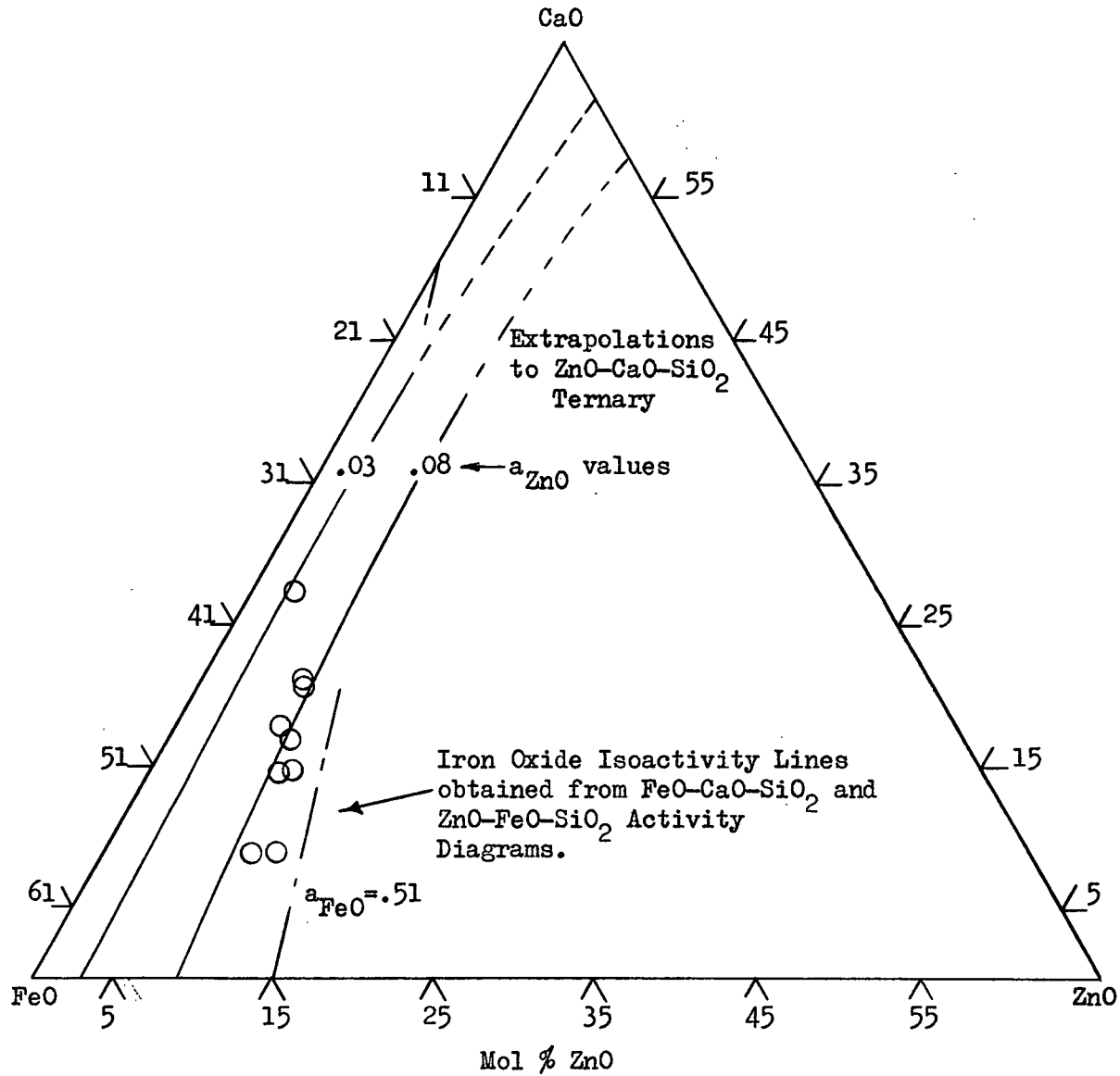


Figure 29. Isoactivity Patterns, ZnO-FeO-CaO-SiO₂ System, 1600°C.

34% SiO₂ Cut

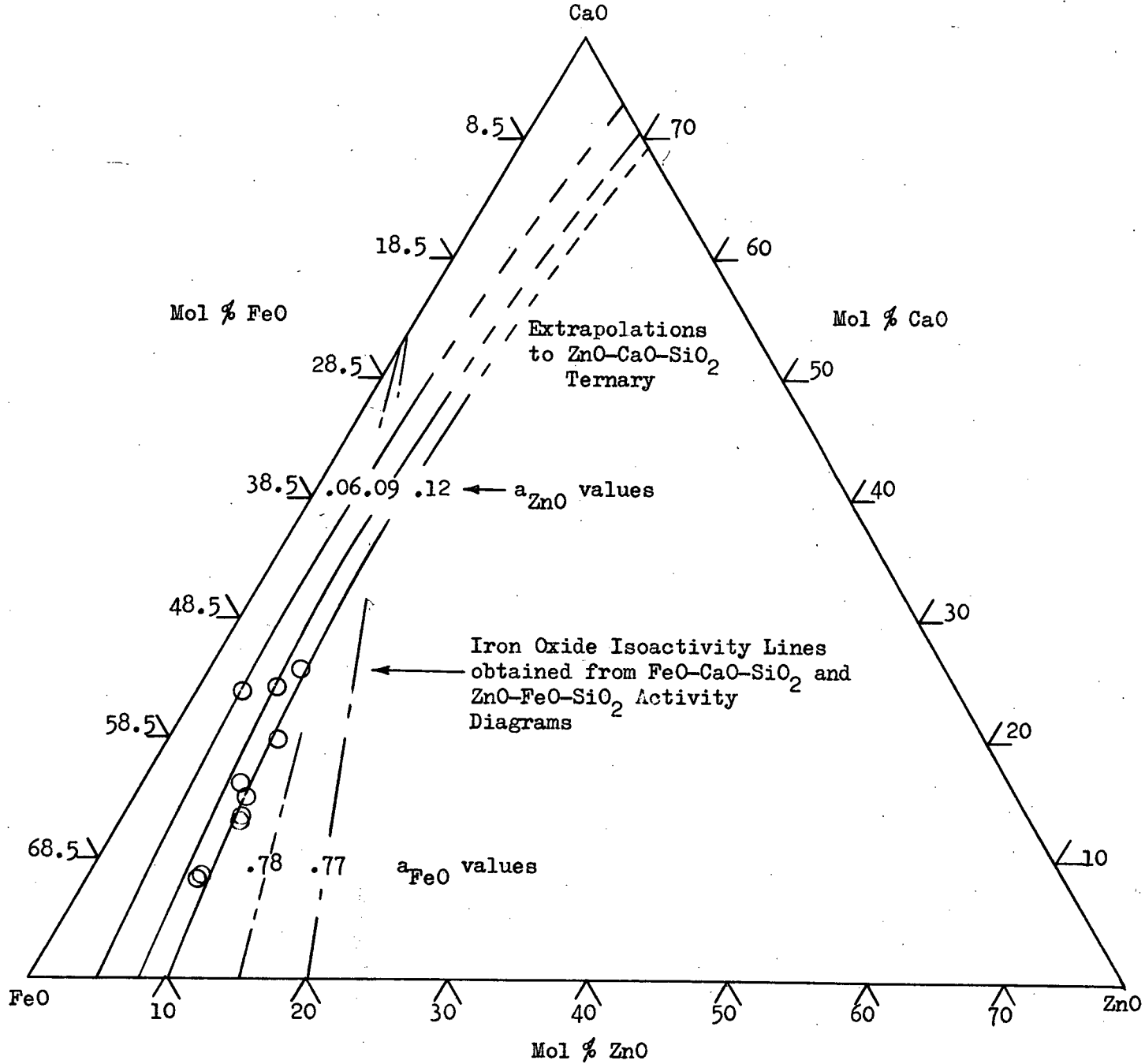


Figure 30. Isoactivity Patterns, ZnO-FeO-CaO-SiO₂ System, 1600°C.
 21.5% SiO₂ Cut

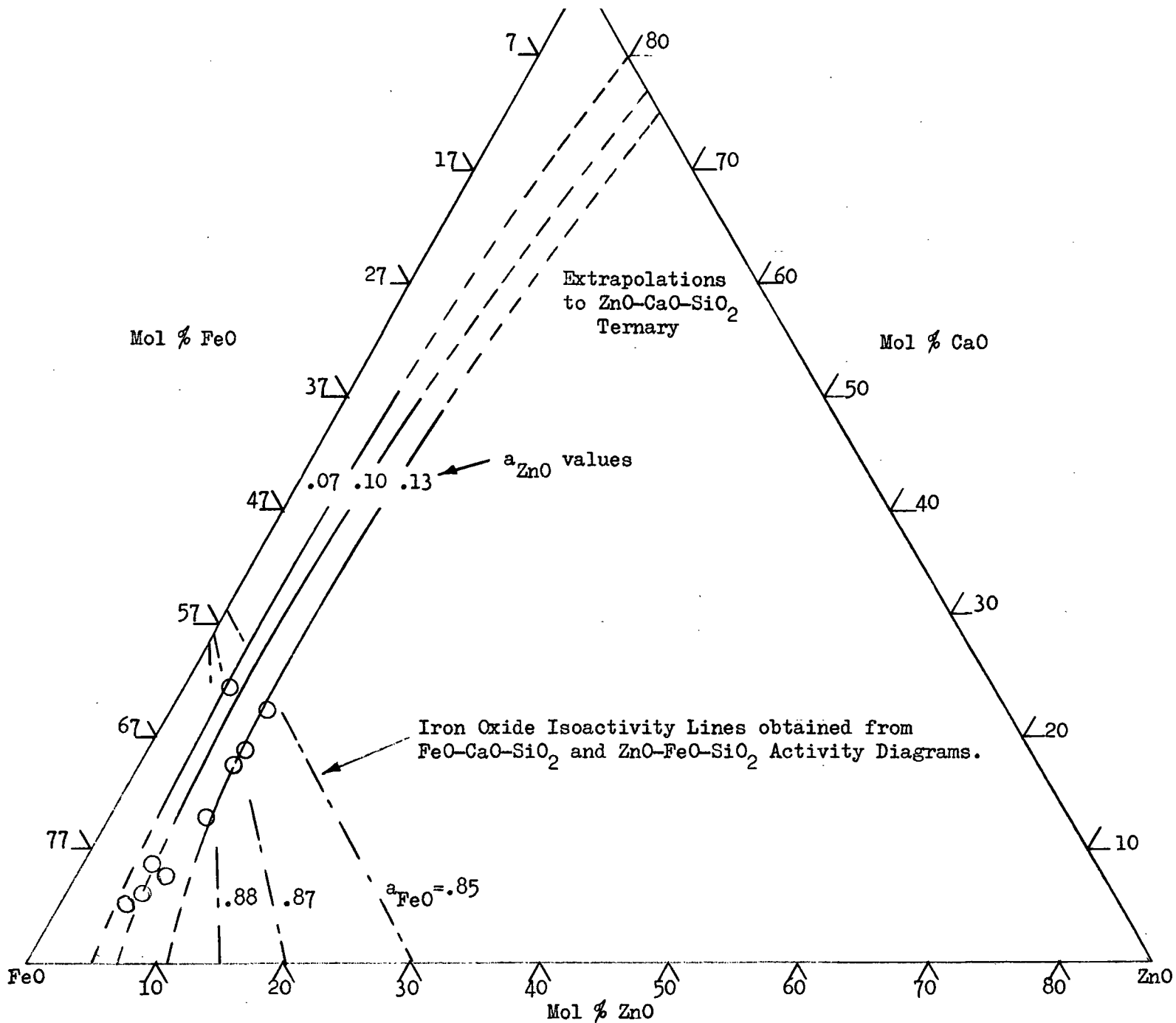


Figure 31. Isoactivity Patterns, ZnO-FeO-CaO-SiO₂ System, 1600°C.

13% SiO₂ Cut

Because of the number of components in the system, no extension or check of the data was possible. The data is presented, therefore, without thermodynamic verification.

COMPARISONS WITH OTHER INVESTIGATIONS

The results of the present investigation were compared with the data of Richards and Thorne⁷, Okunev and Bovykin⁶, and Bell, Turner and Peters⁵.

Comparisons of data were made by interpolating activities on the basis of Figures 15, 28, 29 and 30. Temperature adjustments were accomplished by means of the regular solution model²⁰. Because the activity data of previous investigations is reported with reference to a solid standard state, a liquid standard state adjustment corresponding to a zinc oxide entropy of fusion of 2.85 entropy units was applied.

A. Richards and Thorne⁷

The data of Richards and Thorne are presented in Table 3. Their reported zinc oxide activities are generally lower than the results of the present investigation but are within the suggested accuracy limits.

B. Okunev and Bovykin⁶

Two slag types were studied by Okunev and Bovykin: (i) slags essentially represented by the ZnO-FeO-SiO₂ system, and (ii) multicomponent slags.

Table 3.

Comparison of the Data of Richards and Thorne
and the Results of the Present Investigation

ZnO	Slag Assays (Mol %)			Richards and Thorne a_{ZnO}^*	Present a_{ZnO}^\dagger
	SiO ₂	CaO	FeO		
1.4	33	—	66	.0135	.010
1.5	27	33.5	38	.021	.030
1.5	40	21.5	37	.0165	.015
1.3	24	18	57	.016	.024
1.3	27	18	54	.0145	.021
1.3	34	10.5	53	.0115	.0145
1.6	39	26.5	33	.0185	.018

* Liquid Standard State

† Obtained from Silica Cuts ZnO-FeO-CaO-SiO₂ System and adjusted to 1200°C.

The results of the present investigation were found to be in reasonable agreement with their activity data on the ZnO-FeO-SiO₂ system (Figure 32).

Activity data on the multicomponent slags were compared with the present results on the ZnO-FeO-CaO-SiO₂ system by assuming that: (i) MgO and CaO, and (ii) SiO₂ and Al₂O₃ behave similarly in basic slags. On this basis the present results were found to be higher than the activity data reported by Okunev and Bovykin (Figure 33).

C. Bell, Turner and Peters⁵

The data of Bell, Turner and Peters and the results of the present investigation were found to be in good agreement over the experimental range (Figure 33a). This agreement indicates that the behaviour of their industrial slags is closely approximated by the synthetic slags of this investigation.

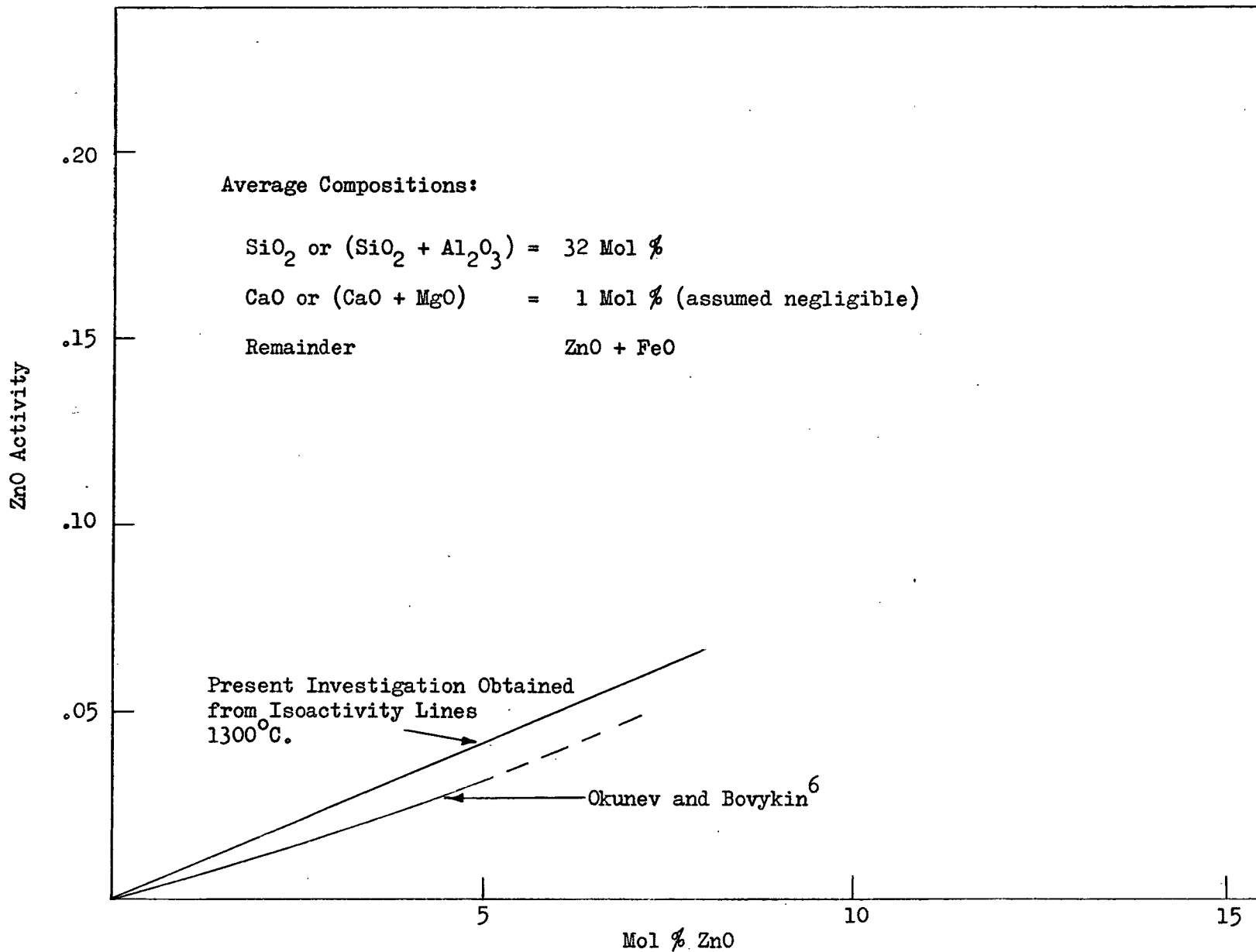


Figure 32. Comparison of Activity Data, ZnO-FeO-SiO₂ System, 1200°C.

Basis: Liquid Standard State.

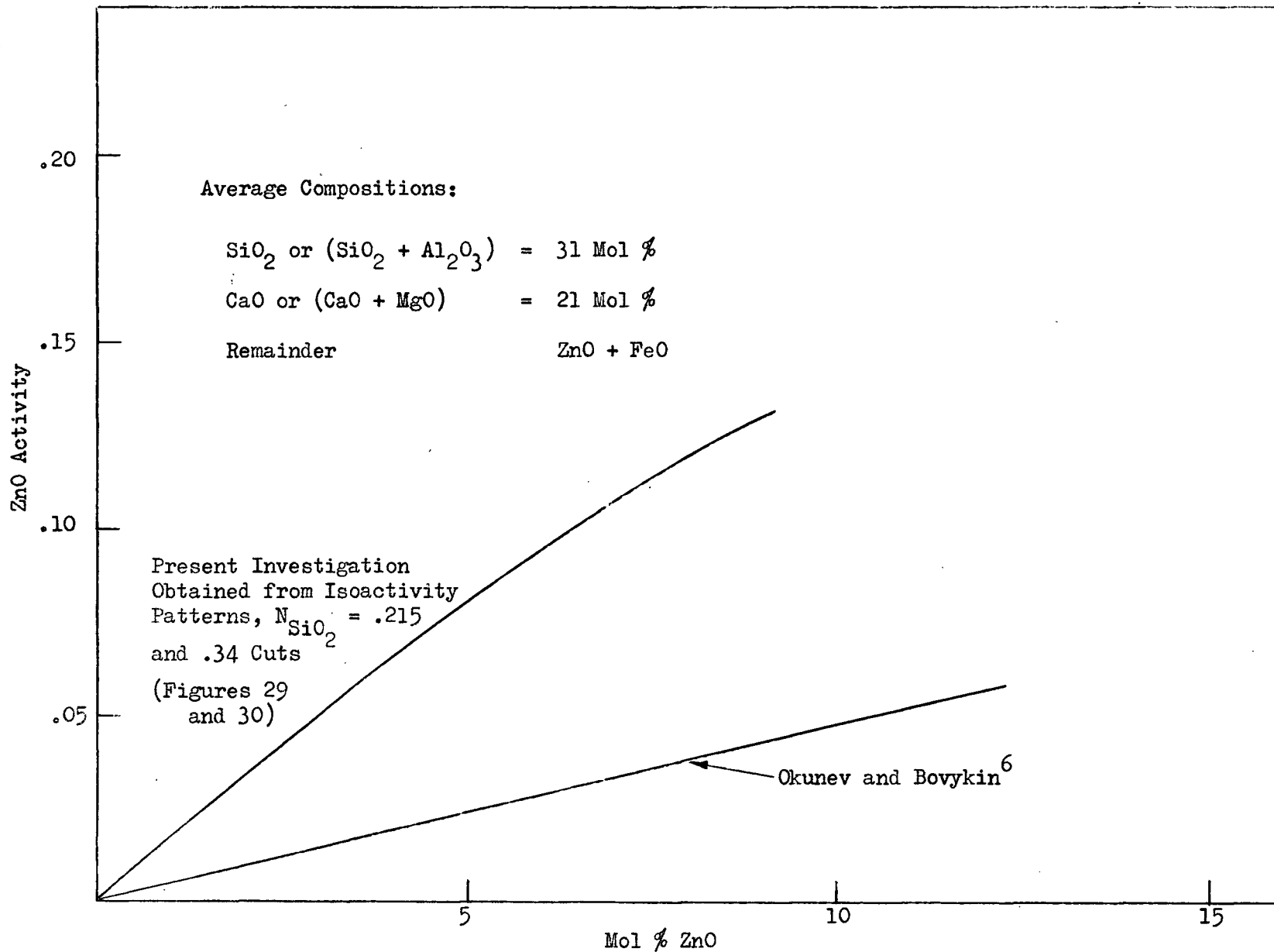


Figure 33. Comparison of Activity Data, ZnO-FeO-CaO-SiO₂ System, 1200°C.

Basis: Liquid Standard State.

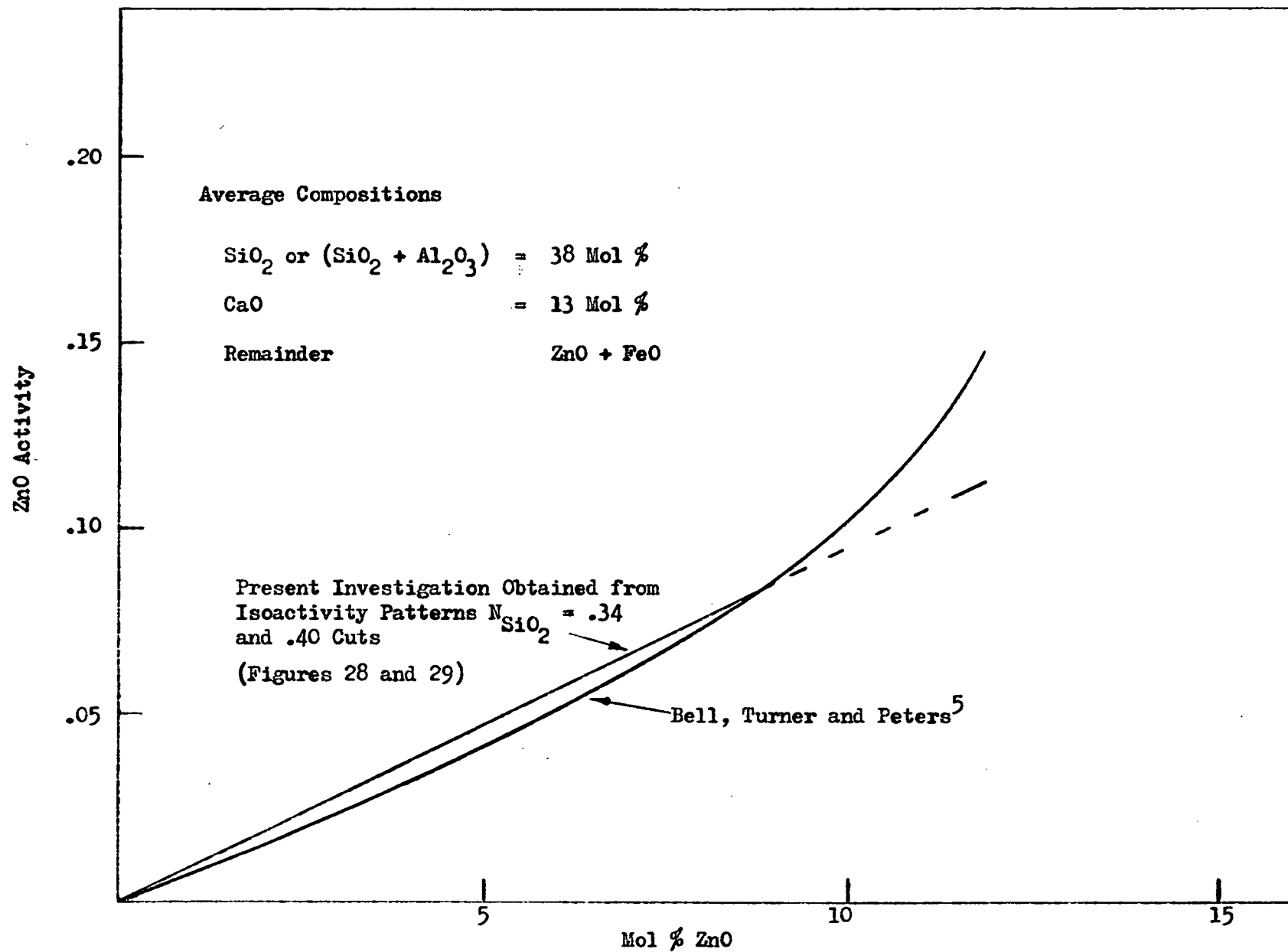


Figure 33a. Comparison of Activity Data, ZnO-FeO-CaO-SiO₂ System, 1200°C.

Basis: Liquid Standard State.

DISCUSSION

Certain inherent problems exist in the measurement of zinc oxide activities. Because of high vapour pressures of zinc, direct oxygen solubility measurement such as those employed in iron oxide and lead oxide determinations are not possible. All investigations (including the present) have had to rely, therefore, on two phase equilibrium measurements for the determination of zinc oxide activities.

The technique used in the present investigation has one major disadvantage. Because the FeO-Fe equilibrium was used to establish the oxygen pressure of the system, the activity of iron oxide in the slag had to be evaluated. In the investigation of the ZnO-FeO-SiO₂ and ZnO-FeO-CaO-SiO₂ systems approximation techniques had to be developed to make the experimental determination of zinc oxide activity possible. Since zinc oxide concentrations were relatively low, information on the component systems could be successfully used in the evaluation of ZnO activities.

The scope of the present investigation was limited to brass compositions which are liquid at 1300°C. Above a zinc activity of .07 the vapour pressure exceeds one atmosphere and boiling occurs. Measurements were limited to zinc oxide compositions corresponding to zinc activities less than this value.

CONCLUSIONS

A slag-metal equilibrium technique has been developed for the measurement of zinc oxide activities in slags. By this method ZnO slags containing FeO were equilibrated with iron saturated brasses. Zinc oxide activities were thus determined in the ZnO-FeO-SiO₂ and ZnO-FeO-CaO-SiO₂ systems, utilizing activities of zinc in the Zn-Cu-Fe system and available information on iron oxide slags.

Thermodynamic analyses of the ZnO-SiO₂ and ZnO-CaO-SiO₂ systems have been carried out using available thermochemical information. Combinations of the experimental and calculated data have produced rigid iso-activity patterns for the systems studied.

The experimental and analytical results are best summarized by reference to Figures 11, 15, 16, 25, and 28 to 31, in which isoactivity patterns for the systems investigated are shown.

The agreement of these results on synthetic slag systems with the industrial data of Bell, Turner and Peters on ZnO-FeO-CaO-SiO₂ type slags, and Okunev and Bovykin on ZnO-FeO-SiO₂ type slags, is reasonable and shows that the present technique of activity measurement provides a good basis for the investigation of zinc oxide activity behaviour in industrial slags.

REFERENCES

1. E. N. Bunting, J. Am. Ceram. Soc.; 13, [1] 8 (1930).
2. E. R. Segnit, J. Am. Ceram. Soc.; 37, [6] 274 (1954).
3. F. D. Richardson, "The Physical Chemistry of Melts", Inst. Min. Met., London (1953) p. 87.
4. J. A. Kitchener and S. Ignatowitz, Trans. Faraday Soc.; 47, 1278 (1951).
5. R. C. Bell, G. H. Turner and E. Peters, J. Metals; 6, 472 (1955).
6. A. I. Okunev and V. S. Bovykin, Proc. of the Academy of Sciences of the U.S.S.R., Chemistry Section, 112, 77 (1957).
7. A. W. Richards and D. J. Thorne, "The Activities of Zinc Oxide and Ferrous Oxide in Liquid Silicate Slags", unpublished.
8. H. H. Kellogg, Eng. and Mining J.; 158, [3] 90 (1957).
9. G. L. Humphrey, E. G. King and K. K. Kelley, U.S. Bureau of Mines Report of Investigations No. 4870 (1952).
10. C. G. Maier, G. S. Parks and C. T. Anderson, J. Am. Chem. Soc.; 48, 2564 (1926).
11. L. H. Everett, P. W. M. Jacobs and J. A. Kitchener, Acta Met.; 5, 281 (1957).
12. J. D. Morris and G. R. Zellars, J. Metals; 8, 1086 (1956).
13. R. Schuhmann, Jr., Acta Met.; 3, 220 (1955).
14. R. Schuhmann, Jr., Acta Met.; 3, 223 (1955).
15. B. N. Daniloff, "Metals Handbook", American Society for Metals (1948).
16. C. Bodsworth and I. M. Davidson, "The Activity of Ferrous Oxide in the FeO-SiO₂ System", to be published.
17. R. Schuhmann, Jr., and P. J. Ensio, J. Metals; 3, 401 (1951).
18. N. A. Gocken and J. Chipman, Trans. A.I.M.E.; 194, 171 (1952).
19. F. D. Richardson, "Physical Chemistry of Melts", Inst. Min. Met., London, (1953) p. 93.
20. J. Chipman, Discussion Faraday Soc.; 4, 23 (1948).

21. Hauffe and Wagner, Z. Elektrochem.; 46, 160 (1940).
22. F. D. Richardson, "The Physical Chemistry of Melts", Inst. Min. Met., London (1953) p. 83.
23. F. C. Langenberg and J. Chipman, Trans. A.I.M.E.; 215, 958 (1959).
24. M. Rey, "The Physical Chemistry of Melts", Inst. Min. Met., London (1953) p. 63.
25. T. B. Winkler and J. Chipman, Trans. A.I.M.E.; 167, 111 (1946).
26. C. R. Taylor and J. Chipman, Trans. A.I.M.E.; 154, 228 (1943).
27. E. T. Turkdogan and J. Pearson, J. British Iron and Steel Inst.; 173, 217 (1953).
28. J. F. Elliot, J. Metals; 6, 485 (1955).
29. G. W. Toop, private communication.

APPENDIX I

Calculations on the Zn-Cu-Fe System

A. Simple Gibbs Duhem Integration

<p>Statement: $Lna_{Zn}^{II} = Lna_{Zn}^I - \int_{a_{Cu}^I}^{a_{Cu}^{II}} \frac{N_{Cu}}{N_{Zn}} dLna_{Cu}$</p> <p>Path: Iron Saturation Line</p>						
Point (Fig. 34)	* a_{Cu}	N _{Cu}	N _{Zn}	∫ _I ^{II}	a _{Zn} (calculated)	* a _{Zn} 1300°C
1	.922	.883	.008		.001	.001
2	.894	.853	.045	2.01	.0065	.0065
3	.830	.809	.100	3.00	.0175	.0170
4	.766	.769	.149	3.54	.030	.030
5	.700	.732	.196	3.91	.046	.047

* From Graphical Integrations

B. Schuhmann's Intercept Integration¹⁴

<p>Statement: $Lna_{Cu} = \left(- \int \left(\frac{\partial N_{Zn}}{\partial N_{Cu}} \right) dLna_{Zn} \right)_{(a_{Zn}, N_{Fe})} \frac{N_{Cu}}{N_{Fe}}$</p> <p>Path: $\frac{N_{Cu}}{N_{Fe}} = 19$</p>					
Point (Fig. 34)	* a _{Zn}	N _{Zn} N _{Cu}	∫ _I ^{II}	a _{Cu} (calculated)	* a _{Cu} 1300°C
A	.0009	.009		.97	.97
B	.0065	.053	.061	.92	.92
C	.017	.125	.152	.84	.85
D	.030	.193	.236	.77	.775
E	.047	.264	.338	.69	.70

* From Graphical Integrations

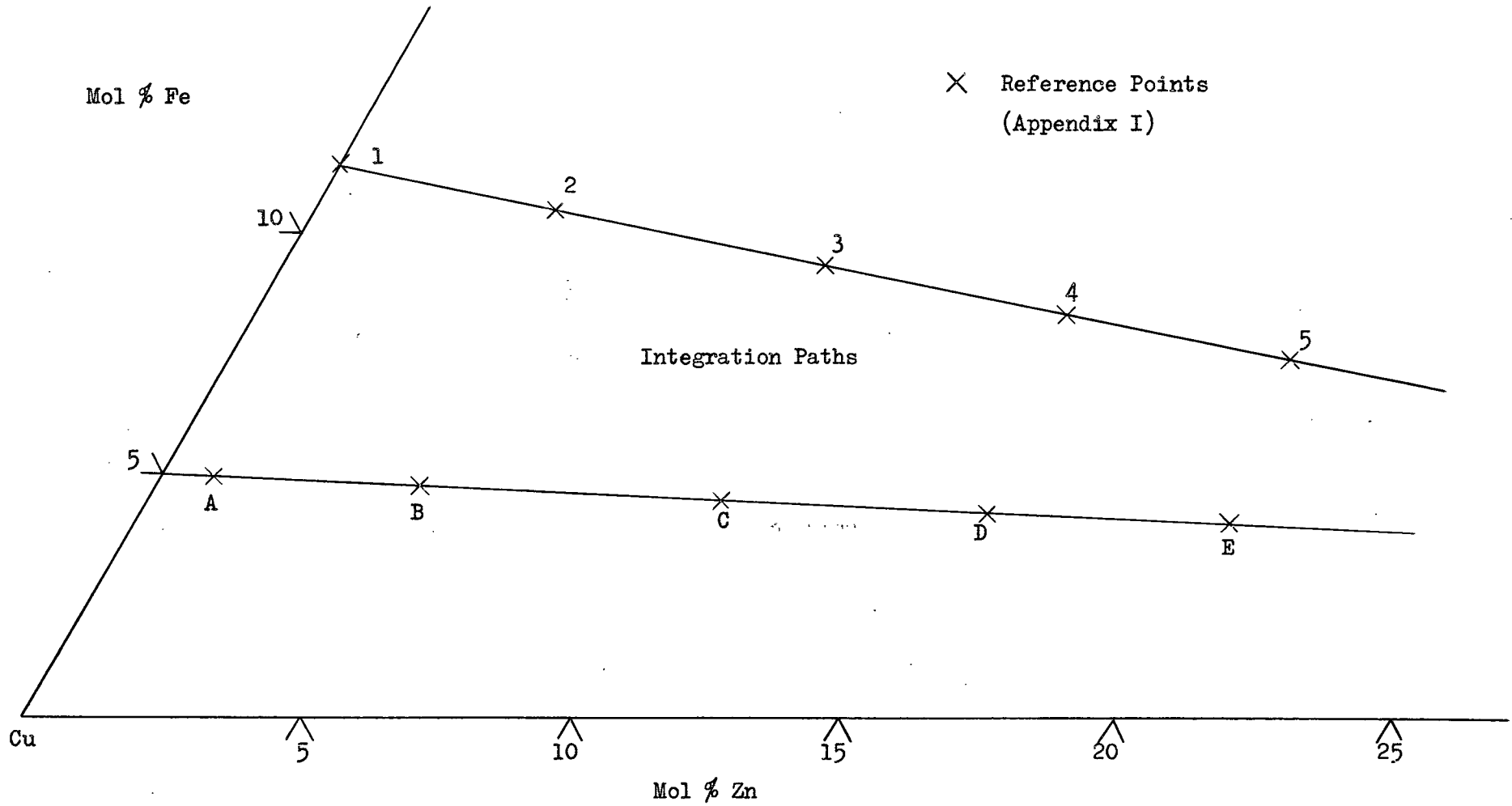


Figure 34. Integration Paths, Zn-Cu-Fe System.

APPENDIX II

Calculation of Activities, System ZnO-SiO₂

A. Liquidus Curve Method²⁰

Statement: $\text{Lna}_{\text{SiO}_2} = - \left(\frac{T - T_{\text{mSiO}_2}}{T} \right) \frac{\Delta S_f (\text{SiO}_2)}{R}$ $\Delta S_f (\text{SiO}_2) = 1.8 \text{ E.U.}$				
N_{SiO_2}	Liquidus Temperature (°K)	$\text{Lna}_{\text{SiO}_2}$	$a_{\text{SiO}_2,T}$	$a_{\text{SiO}_2}^*$ 1613°C
.66	1968	-.00713	.993	.992
.60	1853	-.0559	.946	.918
.55	1753	-.1037	.902	.852
.525	1705	-.1310	.877	.807

* Regular Solution Temperature Adjustment

B. Congruent Melting Point Method²¹

Symbols: ΔH_f = Heat of Fusion of $\text{Zn}_2\text{SiO}_4 = 18.7 \text{ Kcal/mol}$ Θ = Melting Point of $\text{Zn}_2\text{SiO}_4 = 1784^\circ\text{K}$ $x_{\text{ZnO}}, x_{\text{SiO}_2}$ = Compositions of ZnO and SiO ₂ in Zn_2SiO_4 ($x_{\text{ZnO}} = .666, x_{\text{SiO}_2} = .333$) $T, N_{\text{ZnO}}, N_{\text{SiO}_2}$ = Liquidus Temperature, Compositions
Statement: $\text{Lna}_{\text{SiO}_2}^{\text{II}} = \text{Lna}_{\text{SiO}_2}^{\text{I}} + \frac{\Delta H_f}{\Theta} \left\{ \frac{N_{\text{ZnO}} (\Theta - T)}{N_{\text{SiO}_2} - x_{\text{SiO}_2}} + x_{\text{ZnO}} \int_{x_{\text{SiO}_2}}^{N_{\text{SiO}_2}} \frac{(\Theta - T)}{(N - x)_{\text{SiO}_2}^2} d N_{\text{SiO}_2} \right\}$

Appendix II (continued)

N_{SiO_2}	$T^{\circ}K$	$\frac{N_{ZnO}(\Theta - T)}{N_{SiO_2} - x_{SiO_2}}$	$\int_{x_{SiO_2}}^{N_{SiO_2}}$	$a_{SiO_2,T}$	$a_{SiO_2}^*$ 1986
.525	1705	—	—	.877	.807
.525	1705	+ 198	+ 458	.877	.807
.50	1729	+ 168	+ 406	.676	.650
.45	1757	+ 132	+ 306	.45	.450
.40	1775	+ 89.6	+ 201	.305	.314
.35	1784	+ 38.2	+ 60.3	.183	.195
.333	1785	0	0	.140	.154
.300	1784	- 21.2	- 83	.108	.120
Extrapolations from $\frac{\ln^{\delta} SiO_2}{(N_{ZnO})^2}$ Plot (Figure 35)					
.2					.044
.1					.016

* Regular Solution Temperature Adjustment

C. Calculation of a_{ZnO} from a_{SiO_2} Data, Gibbs Duhem Binary Integration (1986°K)

Statement: $\ln^{\delta} ZnO = N_{ZnO} N_{SiO_2} \frac{\ln^{\delta} SiO_2}{(N_{ZnO})^2} - \int_{N_{ZnO}=1}^{N_{ZnO}} \frac{\ln^{\delta} SiO_2}{(N_{ZnO})^2} d N_{ZnO}$					
N_{ZnO}	$\frac{\ln^{\delta} SiO_2}{(N_{ZnO})^2}$	First Term	$\int_{N_{ZnO}=1}^{N_{ZnO}}$	$\ln ZnO$	$a_{ZnO,1986}$
1	- 2.43		0	0	1
.8	- 2.37	+ .379	-.487	-.108	.72
.6	- 0.67	+ .161	-.832	-.671	.31
.4	+ 2.70	-.648	-.636	-1.284	.11
.3	+ 3.90	-.819	-.303	-1.122	.98
.2	+ 5.36	-.858	+ .150	-.708	.98
.1	+ 9.5	-.855	+ .850	-.005	.98
0					0

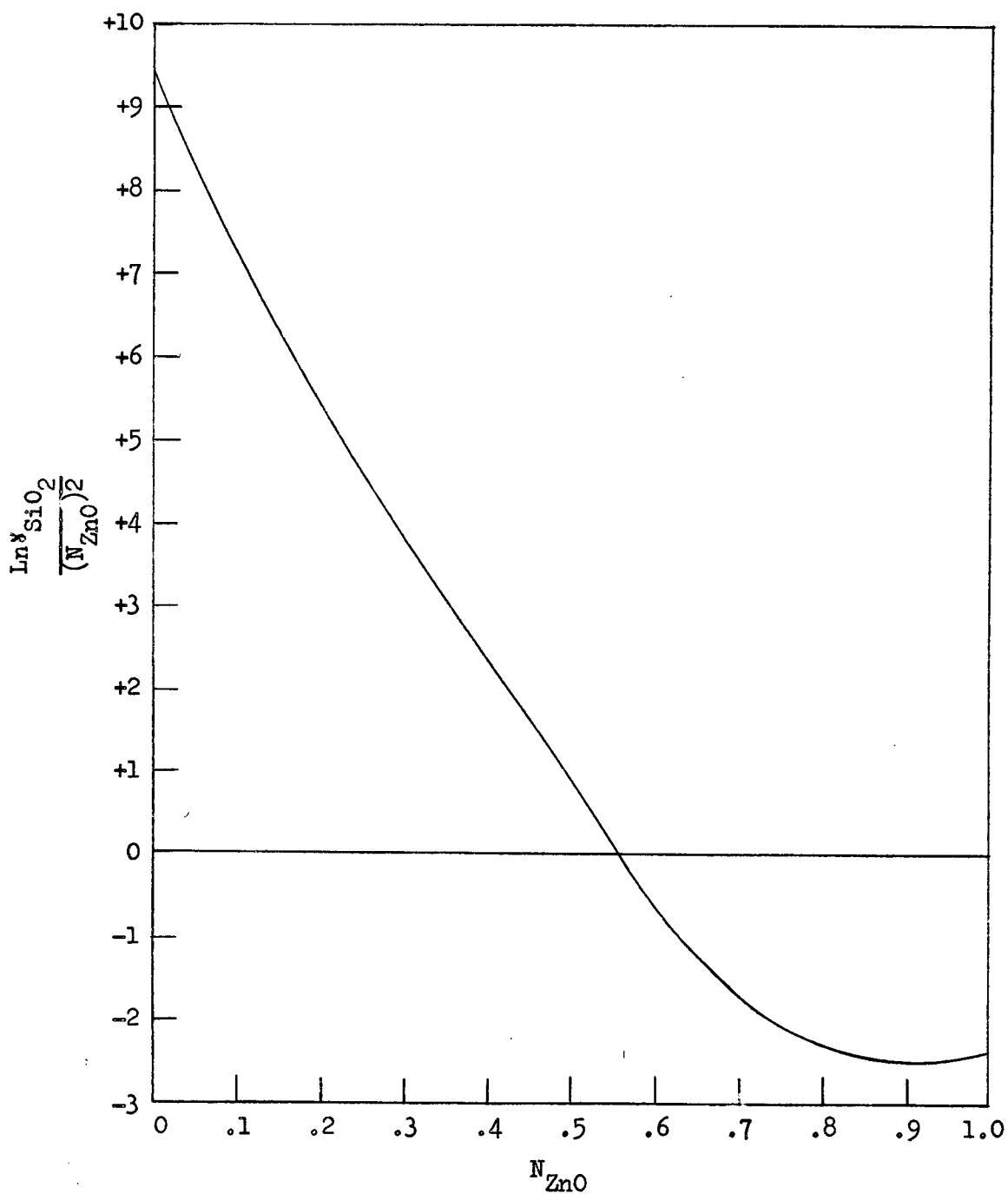


Figure 35. Regular Solution Plot of SiO₂ Activity, System ZnO-SiO₂, 1600°C (used in the calculation of a_{ZnO}).

Appendix II (continued)

D. Tabulation of Activities at 1573°K and 1873°K obtained by Regular Solution Conversion

N_{ZnO}	N_{SiO_2}	a_{ZnO}_{1573}	$a_{SiO_2}_{1573}$	a_{ZnO}_{1873}	$a_{SiO_2}_{1873}$
1	0	1	0	1	0
.9	.1	.87	.008	.875	.012
.8	.2	.70	.029	.72	.04
.7	.3	.47	.11	.50	.117
.6	.4	.26	.295	.295	.31
.5	.5	.13	.70	.165	.66
.4	.6	.08	.946	.10	.95
.3	.7	.073	.946	.09	.96
.2	.8	.073	.946	.10	.96
.1	.9	.073	.946	.10	.96
0	1	0	1	0	1

APPENDIX III

Determination of Zinc Oxide Activities, System ZnO-FeO-SiO₂

A. Activity Coefficient Ratios

Point	<u>Slag Assays</u>			$\frac{N_{FeO}}{N_{ZnO}}$	<u>Metal Assays</u>			a_{Zn}	$\frac{\%ZnO}{\%FeO}$ (1300°C)
	N_{ZnO}	N_{FeO}	N_{SiO_2}		N_{Zn}	N_{Fe}	N_{Cu}		
1	.025	.558	.417	22.32	.051	.100	.849	.0075	.872
2	.040	.536	.423	13.40	.077	.097	.826	.012	.840
3	.046	.544	.409	11.83	.086	.095	.819	.014	.861
4	.067	.512	.420	7.54	.111	.094	.795	.020	.783
5	.071	.506	.422	7.13	.119	.090	.791	.022	.820
6	.044	.566	.390	12.86	.084	.095	.821	.0135	.904
7	.050	.559	.391	11.18	.090	.098	.812	.015	.875
8	.066	.539	.395	8.16	.112	.102	.786	.020	.861
9	.082	.521	.397	6.35	.130	.090	.780	.025	.830
10	.043	.623	.334	14.48	.076	.102	.822	.012	.908
11	.050	.615	.335	12.30	.084	.103	.813	.0135	.867
12	.021	.751	.227	35.76	.044	.105	.851	.006	1.122
13	.027	.747	.224	27.67	.052	.100	.848	.0075	1.080
14	.039	.741	.218	19.00	.073	.104	.823	.011	1.091
15	.049	.730	.219	14.89	.087	.092	.821	.014	1.091
16	.054	.721	.223	13.35	.091	.097	.812	.015	1.044
17	.065	.709	.224	10.91	.105	.102	.793	.0185	1.054

Appendix III (continued)

B. Calculation of Zinc Oxide Activities

Point (see Part A)	$\frac{\delta \text{ZnO}}{\delta \text{FeO}}_{1300^\circ\text{C}}$	a_{FeO} (Thermodynamic Analysis)	γ_{FeO}	γ_{ZnO}	a_{ZnO}
1	.872	.41	.735	.64	.016
2	.840	.40	.745	.63	.025
3	.861	.41	.755	.65	.029
4	.783	.39	.76	.60	.040
5	.820	.39	.77	.63	.045
6	.904	.435	.77	.695	.030
7	.875	.43	.77	.675	.034
8	.861	.42	.78	.67	.0445
9	.830	.41	.785	.655	.054
10	.908	.57	.915	.83	.036
11	.867	.575	.935	.81	.0405
12	1.122	.81	1.08	1.21	.0255
13	1.080	.815	1.09	1.18	.032
14	1.091	.81	1.09	1.19	.047
15	1.091	.805	1.10	1.20	.059
16	1.044	.795	1.10	1.15	.062
17	1.054	.79	1.11	1.17	.076

Thermodynamic Analysis of the ZnO-FeO-SiO₂ System; Calculations

A. Schuhmann's¹⁴ ternary intercept integrations of a_{ZnO} and a_{FeO} were performed along paths as shown in Figure 36.

B. Sample calculation, ternary intercept integration of ZnO activities

<p>Statement: $\text{Lna}_{\text{ZnO}} = \left\{ - \int \left(\frac{\partial N_{\text{SiO}_2}}{\partial N_{\text{ZnO}}} \right)_{(a_1, N_3)} d\text{Lna}_{\text{SiO}_2} \right\}_{N_{\text{ZnO}}/N_{\text{FeO}}}$</p> <p>Path: $\frac{N_{\text{ZnO}}}{N_{\text{FeO}}} = 1$</p>						
Point (Figure 36)	a_{SiO_2}	$\text{Lna}_{\text{SiO}_2}$	$\frac{N_{\text{SiO}_2}}{N_{\text{ZnO}}}$	- ∫	a_{ZnO}	Expected * a_{ZnO}
1	.83	- 0.185	1.25	0	0.10	0.10
2	.73	- 0.315	1.08	0.150	0.115	0.11
3	.60	- 0.51	0.96	0.348	0.140	0.135
4	.38	- 0.97	0.75	0.738	0.21	0.20
5	.25	- 1.39	0.61	1.023	0.28	0.27
6	.16	- 1.83	0.52	1.269	0.35	0.335
7	.10	- 2.30	0.41	1.473	0.435	0.435

* Expected from graphical integrations¹³.

C. Simple Gibbs Duhem integrations were performed along paths as shown in Figure 36.

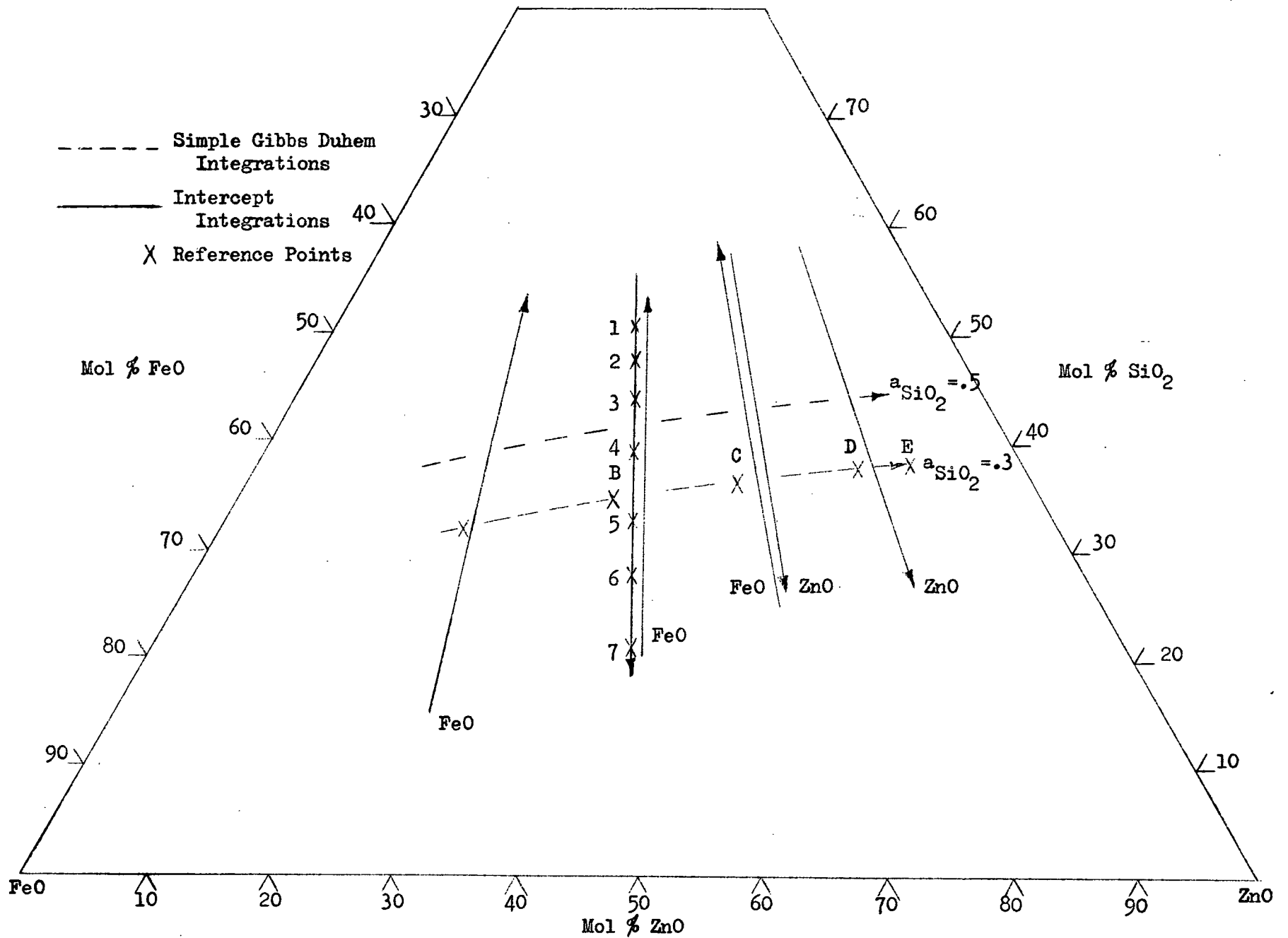


Figure 36. Integration Paths, ZnO-FeO-SiO₂ System.

Appendix IV (continued)

D. Sample Calculation, Simple Gibbs Duhem Integration along a Silica Isoactivity Line.

Statement:
$$\text{Ln}a_{\text{FeO}} = - \int \frac{N_{\text{ZnO}}}{N_{\text{FeO}}} d\text{Ln}a_{\text{ZnO}} \quad (a_{\text{SiO}_2} = \text{constant})$$

Path: $a_{\text{SiO}_2} = .3$

Point (Figure 36)	$\frac{N_{\text{ZnO}}}{N_{\text{FeO}}}$	a_{ZnO}	$\text{Ln}a_{\text{ZnO}}$	\int	a_{FeO}	Expected * a_{FeO}
A	0.39	.16	- 1.83	0	0.55	.55
B	0.86	.23	- 1.47	0.23	0.425	.42
C	1.62	.27	- 1.32	0.19	0.36	.37
D	3.50	.29	- 1.24	0.20	0.29	.30
E	5.60	.30	- 1.21	0.16	0.24	.245

* Expected from ternary intercept¹⁴ and graphical¹³ integrations.

APPENDIX V

Thermodynamic Analysis of the ZnO-CaO-SiO₂ System; Calculations

- A. Schuhmann's ternary intercept¹⁴ and simple Gibbs Duhem integrations were performed along paths as shown in Figure 37.

- B. For examples of integration procedures see Appendix IV.

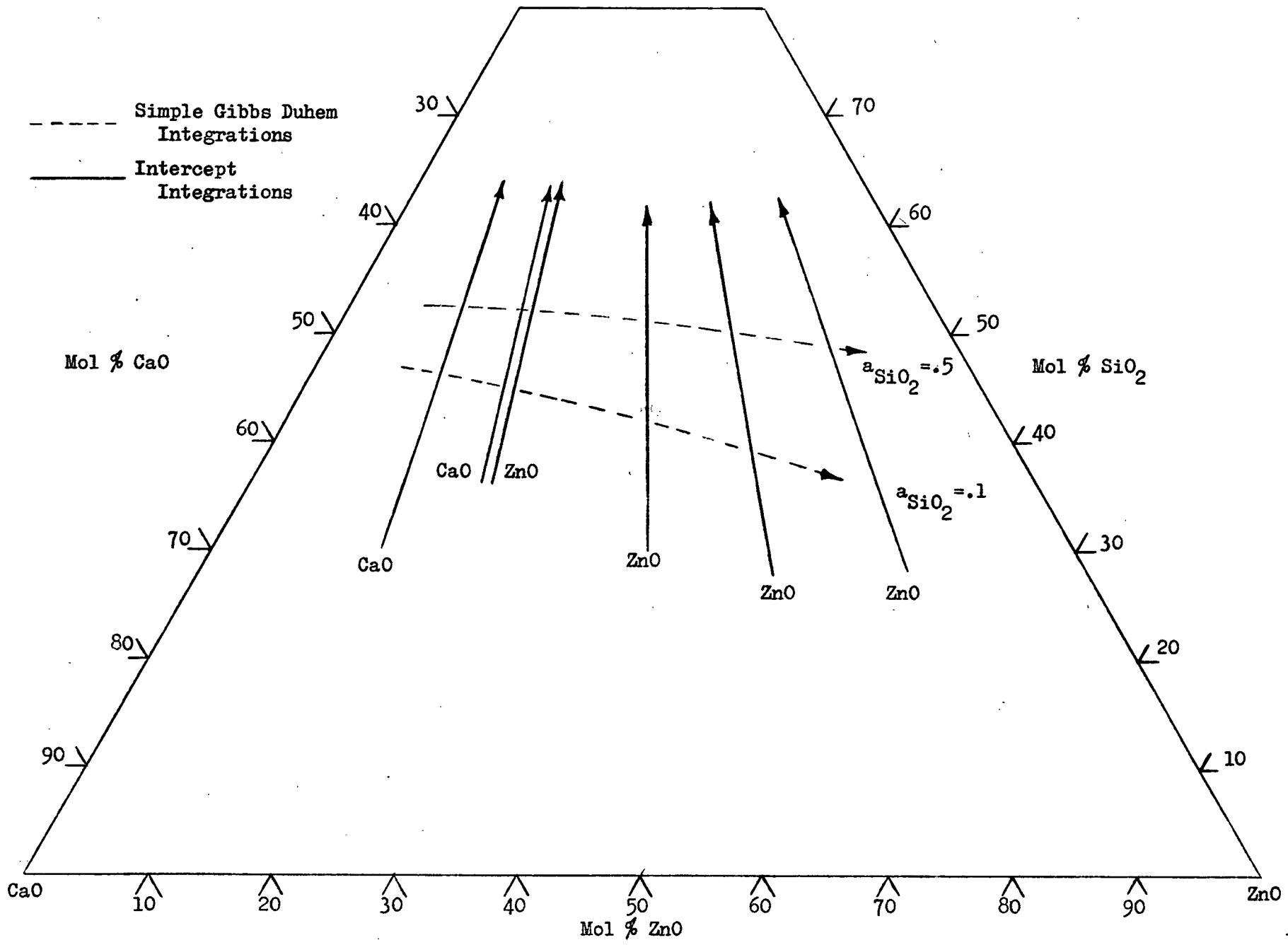


Figure 37. Integration Paths, ZnO-CaO-SiO₂ System.

APPENDIX VI

Determination of Zinc Oxide Activities, System ZnO-CaO-FeO-SiO₂

A. Activity Coefficient Ratios

Point	Slag Assays				$\frac{N_{FeO}}{N_{ZnO}}$	Metal Assays		a_{Zn}	$\frac{\%ZnO}{\%FeO}$ (1300°C)
	N_{ZnO}	N_{CaO}	N_{FeO}	N_{SiO_2}		N_{Zn}	N_{Fe}		
1	.033	.203	.380	.383	11.52	.071	.098	.011	.663
2	.036	.204	.372	.386	10.33	.076	.104	.012	.647
3	.068	.142	.394	.394	5.79	.125	.091	.0235	.710
4	.071	.144	.383	.400	5.39	.125	.089	.0235	.663
5	.093	.079	.411	.417	4.40	.148	.076	.030	.702
6	.0955	.077	.422	.406	4.40	.150	.078	.031	.712
7	.023	.272	.381	.322	16.57	.076	.098	.012	.976
8	.062	.210	.392	.334	6.32	.130	.091	.025	.825
9	.063	.178	.401	.358	6.38	.117	.079	.0215	.715
10	.064	.206	.396	.331	6.18	.145	.085	.029	.934
11	.073	.168	.411	.348	5.63	.144	.082	.0285	.843
12	.077	.146	.437	.338	5.67	.145	.090	.029	.856
13	.087	.148	.425	.338	4.88	.150	.086	.0305	.778
14	.090	.089	.489	.333	5.47	.137	.077	.027	.772
15	.104	.089	.473	.334	4.55	.153	.082	.031	.736
16	.031	.240	.517	.206	16.38	.093	.083	.0155	1.326
17	.052	.246	.480	.222	9.21	.148	.079	.030	1.441
18	.063	.260	.457	.220	7.23	.161	.076	.0335	1.263
19	.069	.164	.566	.200	8.24	.127	.080	.024	1.034
20	.077	.201	.511	.210	6.69	.149	.076	.030	1.049
21	.078	.073	.645	.206	8.27	.127	.100	.024	1.034
22	.080	.151	.565	.204	7.02	.146	.076	.029	1.065
23	.081	.078	.636	.205	7.84	.123	.095	.023	.940
24	.0835	.138	.552	.228	6.73	.146	.074	.029	1.018
25	.0845	.131	.568	.218	6.71	.152	.082	.031	1.086
26	.037	.243	.594	.125	16.19	.099	.123	.017	1.436
27	.052	.051	.766	.131	14.68	.120	.103	.0225	1.723
28	.052	.089	.735	.124	14.22	.120	.102	.0225	1.670
29	.059	.061	.753	.126	12.68	.120	.107	.0225	1.488
30	.070	.074	.723	.134	10.30	.125	.093	.023	1.237
31	.072	.129	.673	.126	9.39	.148	.082	.295	1.434
32	.073	.176	.620	.132	8.49	.146	.079	.029	1.284
33	.074	.188	.603	.136	8.09	.152	.079	.031	1.310
34	.075	.224	.572	.130	7.64	.161	.073	.0335	1.336

Appendix VI (continued)

B. Calculation of Zinc Oxide Activities

Point (see Part A)	$\frac{\% \text{ZnO}}{\% \text{FeO}}_{1300^\circ\text{C}}$	$a_{\text{FeO}}^\dagger_{1600^\circ\text{C}}$	$\% \text{FeO}^*_{1300^\circ\text{C}}$	$\% \text{ZnO}_{1300^\circ\text{C}}$	$a_{\text{ZnO}}^*_{1600^\circ\text{C}}$
1	.663	.46	1.25	.83	.028
2	.647	.46	1.29	.83	.031
3	.710	.45	1.17	.84	.058
4	.663	.45	1.21	.79	.058
5	.702	.45	1.11	.78	.081
6	.712	.45	1.08	.78	.081
7	.976	.55	1.54	1.50	.032
8	.825	.525	1.42	1.17	.072
9	.715	.53	1.39	1.00	.063
10	.934	.525	1.40	1.30	.080
11	.843	.525	1.34	1.13	.081
12	.856	.525	1.24	1.06	.081
13	.778	.52	1.28	1.00	.087
14	.772	.53	1.10	.85	.078
15	.736	.52	1.13	.83	.089
16	1.326	.795	1.66	2.20	.061
17	1.441	.785	1.79	2.58	.118
18	1.263	.775	1.88	2.38	.130
19	1.034	.785	1.48	1.53	.099
20	1.049	.78	1.65	1.73	.123
21	1.034	.79	1.27	1.31	.096
22	1.065	.785	1.49	1.58	.118
23	.940	.79	1.29	1.21	.095
24	1.018	.785	1.52	1.55	.121
25	1.086	.785	1.47	1.60	.125
26	1.436	.86	1.56	2.22	.072
27	1.723	.885	1.19	2.05	.095
28	1.670	.885	1.24	2.07	.095
29	1.488	.885	1.21	1.80	.097
30	1.237	.88	1.27	1.57	.102
31	1.434	.875	1.37	1.96	.127
32	1.284	.865	1.48	1.90	.128
33	1.310	.86	1.52	1.99	.132
34	1.336	.845	1.59	2.12	.141

* Regular Solution Temperature Adjustment

† From Auxiliary Ternary Systems